DOE/ER/40335--5

DE91 000979

THEORETICAL NUCLEAR PHYSICS

Progress Report
for Period October 1, 1989 to October 1, 1990

Peter Dale Kunz

The Regents of the University of Colorado
Boulder, Colorado 80309

October, 1990

Prepared for

THE U.S. DEPARTMENT OF ENERGY
AGREEMENT NO. DE-FG02-87ER40335

CONTENTS

A. 1990 PROGRESS REPORT–October 1, 1989 to October 1, 1990

1. Ground State Correlations of Nuclei in Relativistic Random Phase Approximation J. A. McNeil, C. E. Price and J. R. Shepard

Relativistic (Dirac-equation-based) approaches to nuclear phenomena have enjoyed some successes in recent years and have provided a common framework for understanding nuclear structure and scattering.[1] The simple relativistic mean field approach (QHD-I) bears the closest resemblance to non-relativistic approaches in that the dynamical vacuum is excluded. This model's degrees of freedom include nucleons and two isoscalar mesons, a Lorentz scalar (sigma) and a Lorentz vector (omega). The structure theory has been successfully applied to closed shell nuclei[2], deformed nuclei[3], excited spectra[4], and nuclei near closed shells[5].

In this work we examine the ground state correlations implied by the random phase approximation reported in several recent articles[4]. In this study we have assumed that vacuum fluctuation effects are approximately accounted for in the adjusted meson masses and meson-nucleon coupling constants, and therefore need not be included explicitly. This theory is very similar to standard non-relativistic approaches and we apply the many-body correlation methods of Thouless[6] and others to the present QHD problem.

The specific quantities of interest are 1) the shift in the ground state energy due to correlations, 2) RPA correlation corrections to the charge density, and 3) occupancy and vacancy numbers due to 2p-2h configurations in the correlated ground state. We have calculated these quantities for ^{16}O and ^{40}Ca for which comparisons to previous nonrelativistic calculations are possible (for further details of our calculations see ref. 7). An examination of the isoscalar RPA excitation spectrum in ^{16}O shows that the 1^- and 3^- states are the most affected by the RPA correlations. Therefore the correlation quantities will be dominated by these modes. Calculations including the 2^- and 0^- phonons differ only slightly from those with the 1^- and 3^- only.

In Table I we present several quantities of interest to our correlation study of ^{16}O . We include the 1^- and 3^- phonons up to a 80 MeV. The spurious 1^- is excluded. First note the magnitude of the renormalization factor which measures the overall strength of the correlations. For the RPA to be valid we should have this factor less than unity. The present value, while less than one, is still appreciable indicating that the correlations are fairly strong in this case. Nevertheless we find that the shift in the ground state energy is only -3.22 MeV compared to the Agassi[8] result of -0.408 MeV. It is already well known that Dirac MFT significantly underbinds ^{16}O (by about 2.5 MeV per nucleon). The correlation shift is thus much too small to resolve this discrepancy.

Quantity	Dirac RPA	Agassi[8]
Energy shift	−3.22 MeV	−0.405 MeV
RMS Radius	2.753 fm	--
Normalization	0.598	0.408

Table I. Dirac-RPA Correlation Quantities for ^{16}O

We next examine the ^{16}O ground state charge density. Figure 1 shows the effect of correlations due to the 1^- and 3^- phonons as discussed in the previous paragraph compared to the Dirac-Hartree mean field result and a fourier-bessel fit to the experimental data[9]. As expected, the 3^- phonon correlations remove charge from the interior region and move it to the surface region while the 1^- phonon correlations add some charge to the interior through population of the $2s_{1/2}$ orbital. The net result is a slightly larger root-mean-square radius of 2.753 fm compared to the mean field value of 2.700 fm. The shape of the correlated charge density is not appreciably affected by the correlations.

Table II presents the occupancy and vacancy numbers for ^{16}O compared with the values of Agassi[8]. (These expressions are normalized to the number of particles, not the probability). We find numbers of approximately the same magnitude as Agassi giving a net 0.384 particles removed from the MFT ground state due to correlations compared to Agassi's value of 0.357.

Vacancy Numbers			Occupancy Numbers		
Orbital	Dirac RPA	Agassi[8]	Orbital	Dirac RPA	Agassi[8]
$1s_{1/2}$	0.021	0.019	$1d_{5/2}$	0.200	0.172
$1p_{3/2}$	0.158	0.180	$2d_{5/2}$	0.010	—
$1p_{1/2}$	0.205	0.158	$1d_{3/2}$	0.063	0.082
Sum	0.384	0.357	$2d_{3/2}$	0.028	0.035
			$3d_{3/2}$	0.013	0.015
			Sum	0.314	0.349

Table II. Occupancy and Vacancy Numbers for ^{16}O

In summary, we found that the shift in the ground state energy for both ^{16}O and ^{40}Ca was quite small, only −3.22 MeV for ^{16}O and −2.95 MeV for ^{40}Ca . For the charge densities, in ^{16}O the 1^- and 3^- contributions largely cancel in the interior while for ^{40}Ca the 3^- contribution reduces the central density to give a

reasonable description of the data. We also calculated the occupancy and vacancy numbers for the two nuclei, and where comparisons are available our results agree reasonably with similar nonrelativistic calculations. This is not surprising given the nature of the mean field approximation used in the present Dirac case.

1. B. D. Serot and J. D. Walecka, Adv. Nuc. Phys. **16**, 1 (1986).
2. C. J. Horowitz and B. D. Serot, Nucl. Phys. **A368**, 503 (1981).
3. R. J. Furnstahl, C. E. Price and G. E. Walker, Phys. Rev. **C36**, 354 (1987).
4. R. Furnstahl, Phys Lett. **152B**, 313 (1985); J. R. Shepard, E. Rost, and J. A. McNeil, Phys. Rev. **C40**, 2320 (1989); J. A. McNeil, R. J. Furnstahl, E. Rost, and J. R. Shepard, Phys. Rev. **C40**, 399 (1989).
5. R. J. Furnstahl and C. E. Price, Phys. Rev. **C40**, 1398 (1989); J. A. McNeil, R. D. Amado, C. J. Horowitz, M. Oka, J. R. Shepard and D. A. Sparrow, Phys. Rev. **C34**, 746 (1986); J. R. Shepard, E. Rost, C. -Y. Cheung, and J. A. McNeil, Phys. Rev. **C37**, 1130 (1987).
6. D. J. Thouless, *The Quantum Mechanics of Many-Body Systems*, Academic, New York, 1961.
7. J. A. McNeil, C. E. Price and J. R. Shepard, submitted to Phys. Rev. C.
8. D. Agassi, et al., Nuc. Phys. **A130**, 129 (1969).
9. I. Sick, J. B. Bellicard, J. M. Cavedon, B. Frois, M. Huet, P. Leconte, P. X. Hô, and S. Platchkov, Phys. Lett. **88B**, 245 (1979). Fourier-Bessel fits to the experimental data can be found in H.DeVries, et al., Atom. and Nuc. Data Tables **36**, 521 (1987).

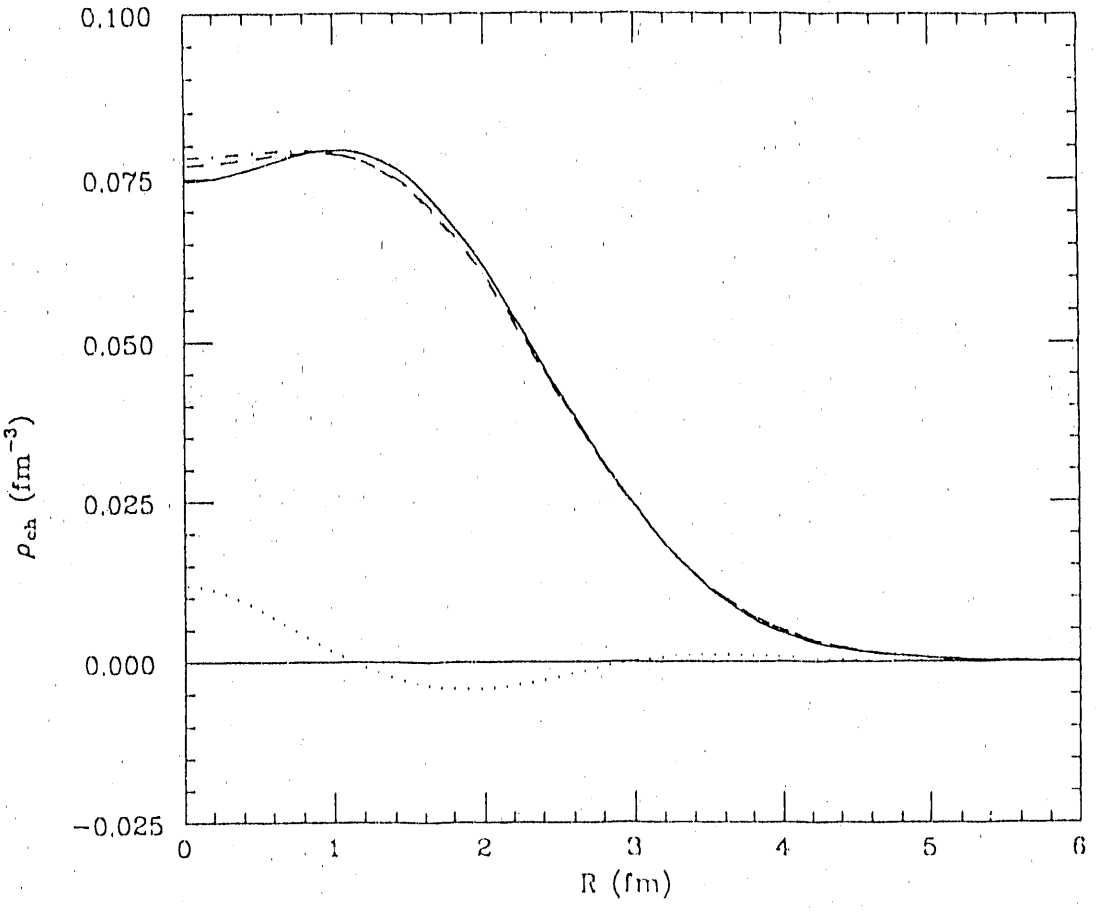

Fig. 1. Charge density of ^{16}O . The solid curve is a Fourier-Bessel fit to the experimental data[9], the dashed curve is the Dirac mean field theory result, the dotted curve is 10 times the correlation correction, and the dash-dot curve is the full correlated charge density.

2. Instability of Infinite Nuclear Matter in the Relativistic Hartree Approximation C. E. Price, J. R. Shepard and J. A. McNeil

The relativistic mean field model obtained from quantum hadro-dynamics[1] (QHD) has been very successful in describing the ground state properties of a wide variety of nuclei.[2] It has also been extensively used as the basis for RPA calculations of nuclear excited state properties[3] and for investigations of scattering processes.[4] An appealing feature of this model is the small number of free parameters. These parameters are the coupling constants of the meson fields (scalar and vector) and the mass of the scalar meson. Generally the coupling constants are fit to the saturation density and binding energy of infinite nuclear matter so that only one parameter remains which can be adjusted to reproduce the properties of finite nuclei. This procedure assumes that the ground state of the infinite system is uniform and may be described in terms of the plane wave solutions of a Dirac equation which includes the uniform meson mean fields.

In our earlier work,[5] we demonstrated that, at the mean-field level of QHD, the uniform nuclear matter ground state may be unstable. Our calculations revealed a lower energy configuration of nuclear matter which contained periodic spatial variations in the nuclear density. We interpreted these density oscillations in terms of nuclear clustering and demonstrated that the instability is sensitive to the value of the scalar (sigma) meson mass. For low values of the sigma mass the nuclear matter ground state is uniform and for high scalar masses (greater than about 690 MeV) nuclear matter crystalizes into alpha particles arranged on a cubic lattice.

In the previous work, we restricted the calculations to the mean-field approximation (which ignores vacuum polarization contributions) and only investigated the dependence on the scalar mass (keeping the vector mass fixed). Since a considerable amount of work has been done in mean-field models which treat the vector (ornega) mass as a parameter[6] and in models which include at least some of the vacuum polarization effects,[7] it is important to determine the range of both meson masses for which the assumed ground state is unstable both with and without vacuum polarization.

To do this, it is most efficient to utilize the random phase approximation (RPA). If the energy of the lowest RPA excited state is less than zero then the assumed ground state is not the lowest energy state of the system, therefore the boundary of the region of instability is marked by the locus of points for which the lowest energy RPA state (assuming a uniform ground state) is at zero excitation. This connection between the RPA and the direct solution was demonstrated in Ref. 5.

We have identified the region of instability for various values of the scalar and vector masses by finding the momentum transfer for which the RPA polarization insertion has a pole at zero excitation energy. The momentum transfer controls the period of the oscillatory structure in the densities of the non-uniform state of nuclear matter (see ref. 5 for details).

The RPA polarization insertion is given by:[8]

$$\Pi^{rpa} = \Pi + \Pi\, D\, \Pi^{rpa} \tag{1}$$

where

$$D_s(q) = 1/[q_\mu^2 - m_s^2 - \Pi_s^{vac}(q)] \tag{2}$$

$$D_v(q) = 1/[q_\mu^2 - m_s^2 - \Pi_v^{vac}(q)] \, . \tag{3}$$

In eq. (1), Π is the usual mean-field polarization insertion (see, for example, ref. 9) and $\Pi^{vac}(q)$ is given by:

$$\Pi_s^{vac}(q) = \frac{3g_s^2}{2\pi^2}\Big\{ M^2 + 3M^{*2} - 4M^*M - \frac{1}{6}q^2 - \int_0^1 d\alpha \, \left[M^{*2} - \alpha(1-\alpha)q^2\right] \ln\Big(\frac{M^{*2} - \alpha(1-\alpha)q^2}{M^2}\Big)\Big\} \tag{4}$$

and

$$\Pi_v^{vac}(q) = \frac{g_v^2 q^2}{\pi^2} \int_0^1 d\alpha \; \alpha(1-\alpha) \ln\Big(\frac{M^{*2} - \alpha(1-\alpha)q^2}{M^2}\Big) \tag{5}$$

where we have assumed that the isospin degeneracy of the vacuum is two. The difference between MFT and RHA is that for MFT the $\Pi_{s,v}^{vac}$ are set to zero in order to eliminate the vacuum contributions.

In uniform nuclear matter only the ratios g_s^2/m_s^2 and g_v^2/m_v^2 enter; so, as we vary the meson masses, we keep these ratios fixed. This insures that the nuclear matter saturation properties (in the uniform state) do not change. If we wished to examine the detailed structure of the non-uniform solution it would be necessary to refit the parameters (in the non-uniform state) for each choice of m_s and m_v.

In fig. 1, we show two views of the boundary of the region for which the uniform ground state of nuclear matter in the mean-field approximation is unstable. Below this surface there is a non-uniform state characterized by density fluctuations of frequency q which has lower energy than the spatially uniform state. Clearly, for the lower values of the scalar mass that are typically used in MFT (*e.g.* 550 MeV) the uniform state is stable for a wide range of vector masses; however, as the scalar mass increases the instability is present for increasingly larger values of the vector mass. Also the value of q for which the uniform state is most unstable is roughly 1.6 times the fermi momentum ($k_F = 1.3$ fm^{-1}) and is only slightly dependent on the meson masses. By taking a cut through the surface in fig. 1 at $m_v = 783$, the results shown in our previous paper[5] can be obtained.

This same surface, obtained from calculations in the relativistic Hartree approximation, is shown in fig. 2. The most striking difference is that the RHA uniform state is stable for all values of the vector mass greater than about 400

MeV regardless of the value of the scalar mass. This can be understood by considering eqs. (2) and (3). The "effective ranges" of the scalar and vector interactions are not controlled solely by the corresponding masses as they are in the mean-field limit. The inclusion of the of the vacuum polarization leads to effective masses for the scalar and vector fields that are given by:

$$m_s^{eff} = \sqrt{m_s^2 + \Pi_S^{vac}}\,, \qquad m_v^{eff} = \sqrt{m_v^2 + \Pi_V^{vac}} \tag{6}$$

and depend on q. The vacuum polarization insertions in eq. (6) are generally less than zero and roughly scale with the corresponding masses. This means that for a given change in the "bare" meson masses, the effective meson masses change much less. Thus, in contrast to the MFT, the RHA-RPA polarization insertion (and hence the onset of the instability) is relatively insensitive to moderate changes in the meson masses.

The results from the RHA indicate that the problem of the instability of nuclear matter is much less severe than for MFT; however, that cannot be interpreted to mean that the instability can be ignored. Even in regions where the RHA uniform ground state is stable, the nearby instability can still effect calculations in finite nuclei. While it is true that the farther the meson masses are from the region of instability the less pronounced the effects on finite nuclei will be, it is by no means obvious that the effects can be entirely eliminated. In fact, it is likely that the subtle structure seen in the interior of nuclei using the standard RHA parameters can be interpreted as a reflection of the nearby non-uniform state of nuclear matter.

Clearly, care must be taken when analyzing any calculation that relies on the assumption that infinite matter is uniform. Specifically, for calculations in both MFT and RHA it is probably unwise to adjust the coupling constants so that the saturation properties of *uniform* infinite nuclear matter are reproduced. A better procedure would be to fit the MFT and RHA coupling constants directly to the bulk properties of finite nuclei.

1. B. D. Serot and J. D. Walecka, Adv. in Nucl. Phys. **16**, 1 (1986).
2. C. J. Horowitz and B. D. Serot, Nucl. Phys. **A368**, 503 (1981); R. J. Furnstahl, C. E. Price and G. E. Walker, Phys. Rev. **C 36**, 2590 (1987); Y. K. Gambhir and P. Ring, Phys. Lett. **202B**, 5 (1988); R. J. Furnstahl and C. E. Price, Phys. Rev. **C 40**, 1398 (1989); U. Hofmann and P. Ring, Phys. Lett. **214B**, 307 (1988).
3. J. R. Shepard, E. Rost and J. A. McNeil, Phys. Rev. **C 40**, 2320 (1989); R. J. Furnstahl, Phys. Lett. **152B**, 313 (1985); P. G. Blunden and P. McCorquodale, Phys. Rev. **C 38**, 1861 (1988).
4. L. G. Arnold, B. C. Clark, R. L. Mercer and P. Schwandt, Phys. Rev. **C 23**, 1949 (1981); J. R. Shepard, E. Rost, E. R. Siciliano, and J. A. McNeil, Phys. Rev. **C 29**, 2243 (1984).
5. C. E. Price, J. R. Shepard and J. A. McNeil, Phys. Rev. **C** (in press).

6. P.-G. Reinhard, M. Rufa, J. Maruhn, W. Greiner and J. Friedrich, Zeit. Phys. **A323**, 13 (1986).
7. C. J. Horowitz and B. D. Serot, Phys. Lett. **140B**, 181 (1984).
8. C. J. Horowitz and J. Piekarewicz, Phys. Rev. Lett. **62**, 391 (1989).

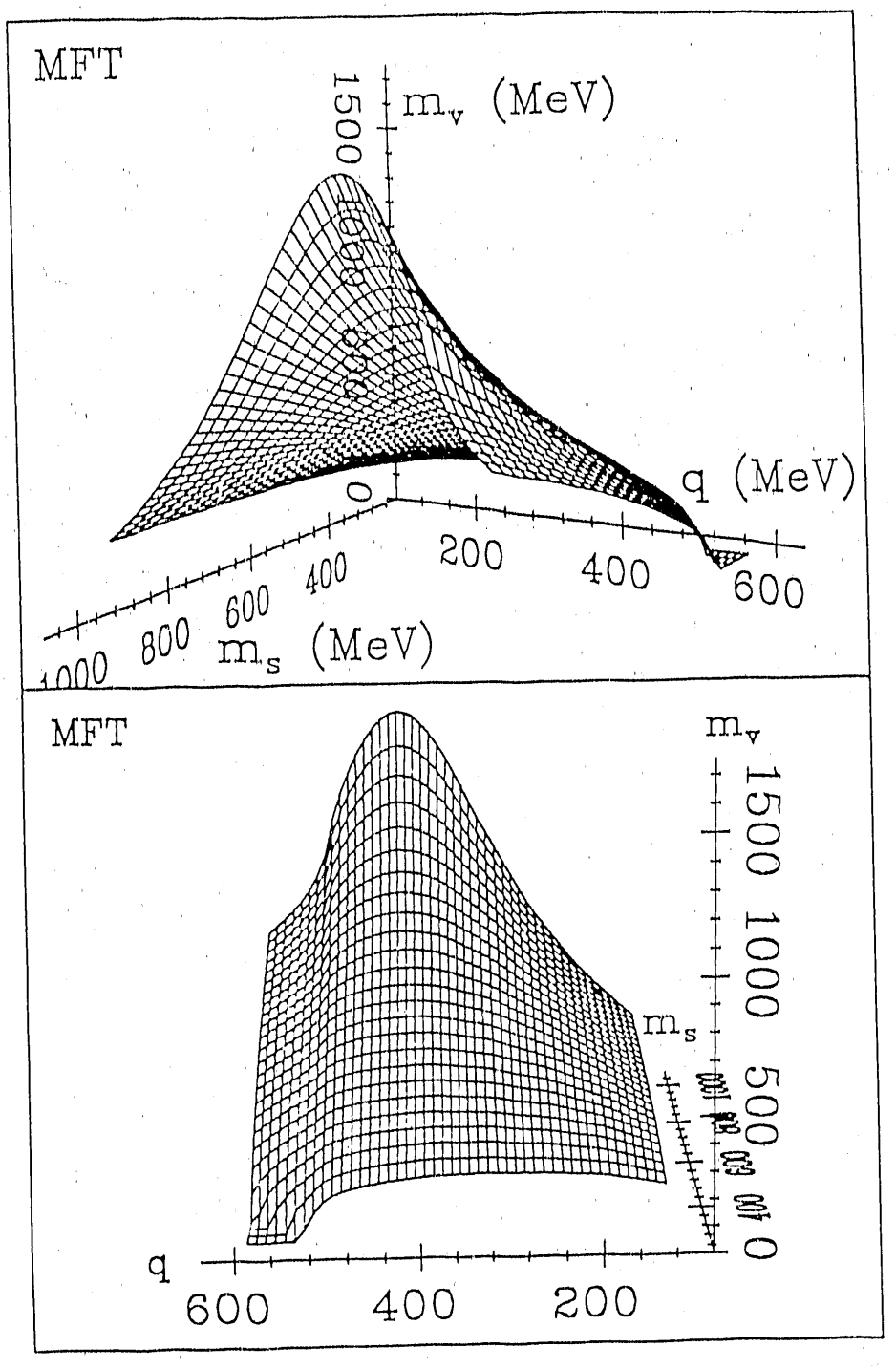

Fig. 1. The region of instability of uniform nuclear matter in the mean-field approximation (MFT) as a function of the scalar and vector masses and the frequency. The region below the surface marks the area in which the uniform state is not the lowest energy state of the system as determined in the RPA. For clarity, the upper and lower panels show the same surface from different viewpoints.

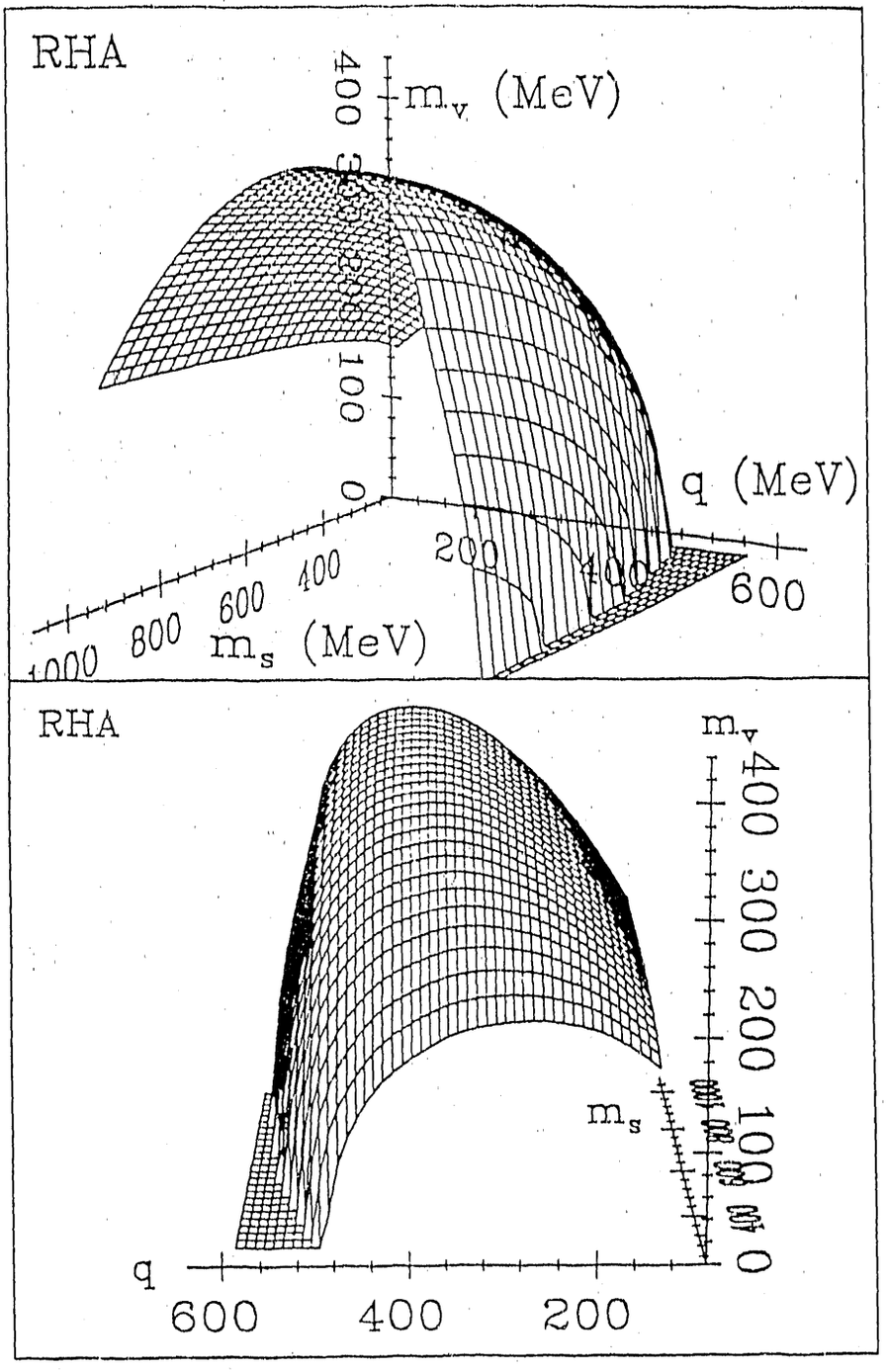

Fig. 2. The region of instability of uniform nuclear matter in the relativistic Hartree approximation (RHA) as a function of the scalar and vector masses and the frequency. The region below the surface marks the area in which the uniform state is not the lowest energy state of the system as determined in the RPA. For clarity, the upper and lower panels show the same surface from different viewpoints.

3. Charge Density Differences for Nuclei Near ^{208}Pb in Relativistic Models C. E. Price and R. J. Furnstahl

There are recent data [1,2] on the charge densities of various nuclei near ^{208}Pb (*e.g.* ^{206}Pb, ^{205}Tl and ^{204}Hg). The difference between the charge densities of two such nuclei that differ by one or two protons should be dominated by the charge density associated with the last occupied proton orbital. For these nuclei near ^{208}Pb, the last occupied proton state is the $3s_{1/2}$ orbital, which has a characteristic two node shape with a large central maximum. This shape should provide a unique signature for the effects of this orbital in the charge density difference, and should make it possible to identify any deviations from the pure single particle picture.

There are at least two effects that are expected to cause the charge density difference to deviate from the pure $3s_{1/2}$ shape. First, the removal of even a single proton will induce some polarization in the remaining core orbitals so that the charge densities of the cores of two neighboring nuclei (like ^{205}Tl and ^{206}Pb) will not cancel exactly. Secondly, the occupation numbers of the least bound proton orbitals need not be identical for these heavy nuclei. For example, rather than being dominated by the removal of a single proton (or pair of protons) from the $3s_{1/2}$ orbital, the charge density difference may be primarily due to the removal of a "fraction" of a proton from each of the $3s_{1/2}$ and $2d_{3/2}$ orbitals (or any more complicated fractional level occupation schemes).

In this work, we study the charge densities of ^{206}Pb, ^{205}Tl and ^{204}Hg in the context of quantum hadro-dynamics[3](QHD). This model has been very successful in describing a wide range of nuclear ground state properties throughout the periodic table, and typically provides agreement with experiment that is on the same level as that obtained using non-relativistic Skyrme interactions.[4] For these calculations, we have used both linear (L) and nonlinear (NL) parametrizations of QHD.

Figure 1 shows the charge density differences for ^{206}Pb$-^{205}$Tl and ^{206}Pb$-^{204}$Hg. In both cases the general shape of the calculated density difference is similar to that of the experiment; however, the calculations overestimate the size of the oscillatory structure. This overestimation is particularly evident in the central maximum where the calculations are two to three times larger than the experiment. This central difference strongly suggests that either core polarization or fractional level occupancies are playing an important role in the charge density differences. The calculations shown in fig. 1, are very similar to those obtained from non-relativistic Hartree-Fock calculations using phenomenological effective interactions (see ref. 1 for ^{205}Tl and ref. 2 for ^{204}Hg). In these earlier calculations both core polarization and fractional level occupancy had significant effects on the charge densities.

In order to demonstrate the effect of core polarization, we will focus on ^{206}Pb and ^{205}Tl. Fig. 2 shows the charge density difference obtained from experiment (solid line) along with two results obtained from the linear model. The dashed line shows the full calculation (as in fig. 1) and the dotted curve shows the charge

density contribution of the $3s_{1/2}$ proton orbital of ^{206}Pb. These two calculations would be identical if the core polarization was negligible. Clearly, there is about a 10% difference at r=0 that persists to all r. Notice that the pure $3s_{1/2}$ result lies above the full calculation, indicating that the core polarization has already reduced the discrepancy with experiment. This reduction actually arises from two distinct sources. First, the absence of the valence $3s_{1/2}$ proton in ^{205}Tl effectively reduces the size of the potential well that is seen by the remaining core orbitals. These orbitals then have a slightly different spherical distribution than the corresponding levels in ^{206}Pb. This accounts for roughly two thirds of the core polarization seen in fig. 2. The remainder arises from the deformation of the ^{205}Tl core. Since removing a single proton leaves an incomplete outer shell, ^{205}Tl is not constrained to have a spherical shape. The calculation shown in fig. 2 (dashed line) allows for the possibility of $L = 1$, 2, and 3 deformations of the ^{205}Tl core (higher deformations were observed to be unimportant), and these deformations contribute one third of the total core polarization effect. Most importantly, notice that while the core polarization does move the calculations away from the pure $3s_{1/2}$ result, it does not begin to explain the large discrepancy with experiment.

In order to understand the discrepancy, we now consider the effects of fractional level occupancy. Since we are only interested in the charge density *differences*, it is sufficient to leave the level filling of ^{206}Pb fixed and only vary the occupancy of the least bound levels in either ^{205}Tl or ^{204}Hg. In figs. 3 and 4, we show the charge density differences for ^{206}Pb$-^{205}$Tl and ^{206}Pb$-^{204}$Hg obtained by varying the occupancy of the high lying proton orbitals. For these calculations, we have assumed that the neutron occupancies are not affected and that the changes in the proton occupancies are restricted to the $3s_{1/2}$ and $2d_{3/2}$ shells.

For ^{206}Pb$-^{205}$Tl, we used the occupancies suggested by Frois's[1] comparison of the experimental results with the mean-field calculations of Campi et al.[5] Specifically, there are 0.7 protons removed from the 3s shell and 0.3 protons removed from the 2d shell. This level occupancy is minimally sufficient to bring our QHD results into agreement with the experimental density. Our central maximum is still slightly too high and the oscillatory structure remains slightly enhanced. The agreement could be improved by using depletions of 0.6 and 0.4 for the 3s and 2d levels respectively. This larger 3s occupancy is supported by the theoretical calculation of Pandharipande[6] in which the occupation probabilities of shell-model orbits in the lead region are estimated by the addition of random-phase approximation corrections to nuclear matter results.

For ^{206}Pb$-^{204}$Hg, we have used the occupancies suggested in ref. 2, based on the average of the occupation numbers required to bring three separate non-relativistic calculations into agreement with experiment. Namely, $\sim$ 1.0 proton removed from the 3s orbital and $\sim$ 1.0 proton removed from the 2d orbital (this corresponds to a fractional occupancy of 0.5 for each of the $3s_{1/2}$ levels). Again this occupancy is sufficient to bring our results into minimal agreement with experiment, but the agreement could be improved by removing slightly fewer protons from the 3s level. Since the three calculations of ref. 2 had a spread of about $\pm$10%,

such a reduction would still be consistent with the non-relativistic calculations. It is important to point out that, particularly for an even-even nucleus like ^{204}Hg, the fractional occupation of the levels near the Fermi surface should be included via the pairing approximation as has been used by Ring et al.[7] rather than by the simple occupation number variation that we have employed here. While it is not expected that the pairing effects would alter the qualitative features of our results, it is likely that the simple picture of the charge density difference in terms of only two levels (the 3s and 2d) would be changed.

1. B. Frois, J. M. Cavedon, D. Goutte, M. Huet, Ph. Leconte, C. N. Papanicolas, X.-H. Phan, S. K. Platchkov, S. E. Williams, W. Boeglin and I. Sick, Nucl. Phys. **A396**, 409c (1983).
2. A. Burghardt, PhD Thesis, University of Amsterdam. ????
3. B. D. Serot and J. D. Walecka, Adv. in Nucl. Phys. **16** (Plenum, New York, 1986).
4. C. J. Horowitz and B. D. Serot, Nucl. Phys. **A368**, 503 (1981); S. J. Lee *et al.*, Phys. Rev. Lett. **57**, 2916 (1986); **59**, 1171 (1987); C. E. Price and G. E. Walker, Phys. Rev. **C36**, 354 (1987); W. Pannert, P. Ring, and J. Boguta, Phys. Rev. Lett. **59**, 2420 (1987); R. J. Furnstahl, C. E. Price, and G. E. Walker, Phys. Rev. **C36**, (1987) 2590; U. Hofmann and P. Ring, Phys. Lett. **214B**, 307 (1988).
5. X. Campi and D. W. L. Sprung, Nucl. Phys. **A194**, 401 (1972).
6. V. R. Pandharipande, C. N. Papanicolas and J. Wambach, Phys. Rev. Lett. **53**, 1133 (1984).
7. Y. K. Gambhir and P. Ring, Phys. Lett. **B202**, 5 (1988) and references therein.

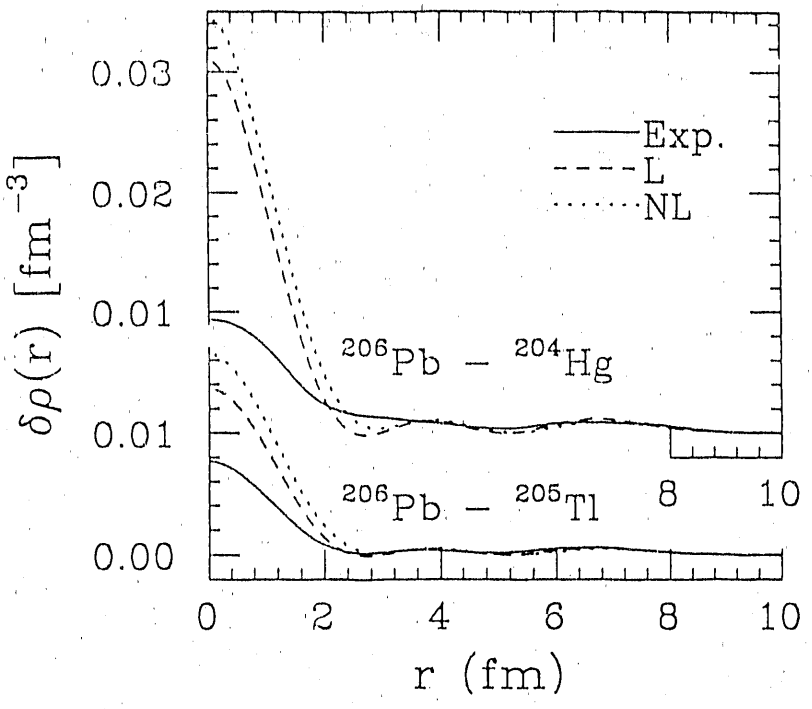

Fig. 1. Charge density differences for ^{206}Pb−^{205}Tl and ^{206}Pb−^{204}Hg. Solid lines are the experimental result, dashed lines are from the linear QHD model and the dashed-dotted lines are from the nonlinear version of QHD.

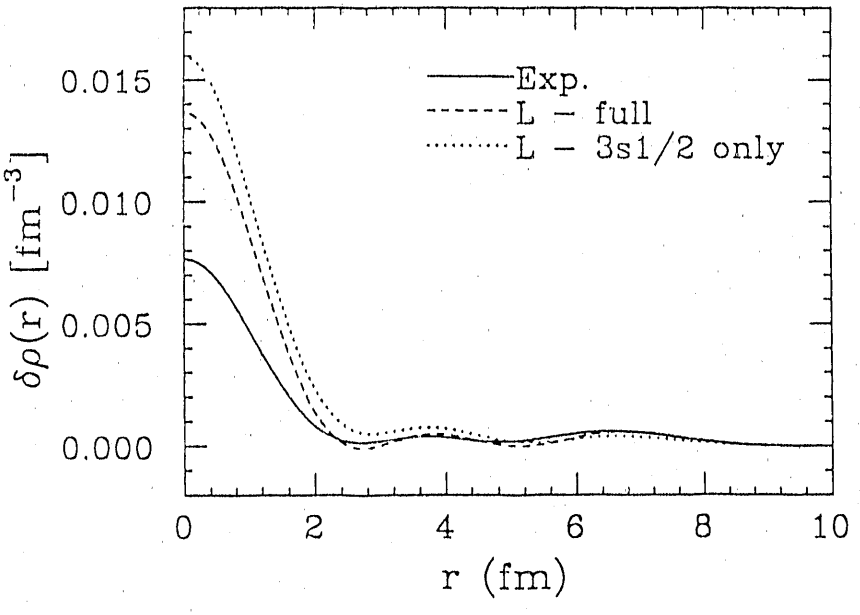

Fig. 2. Core polarization effects in the ^{206}Pb−^{205}Tl charge density difference. The pure $3s_{1/2}$ contribution from ^{206}Pb (dotted) is contrasted with the full calculation (dashed) and experiment (solid).

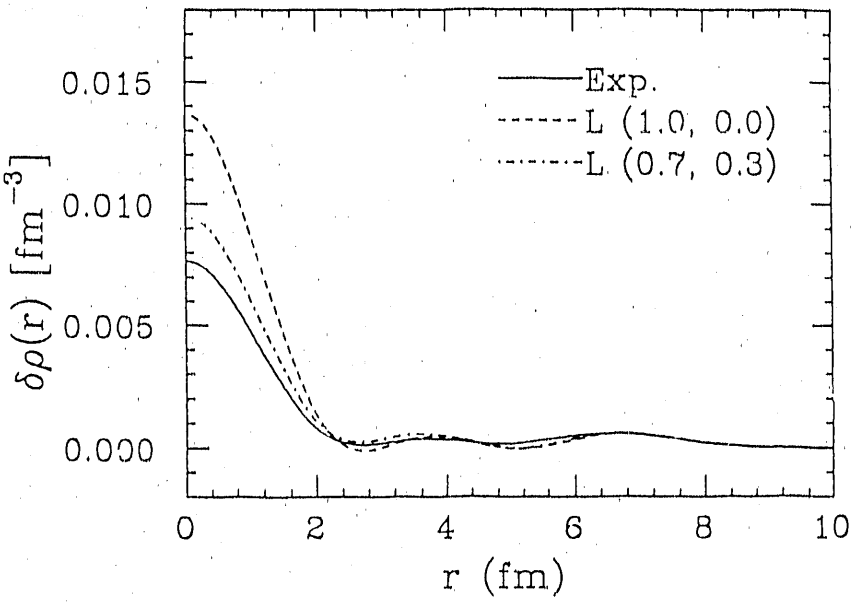

Fig. 3. Effects of fractional level occupancy on the ^{206}Pb−^{205}Tl charge density difference. The solid curve is the experimental result, the other curves are based on the linear version of QHD with (dashed) 1.0 proton removed from the 3s level and (dashed-dotted) 0.7 protons removed from the 3s level and 0.3 from the 2d level.

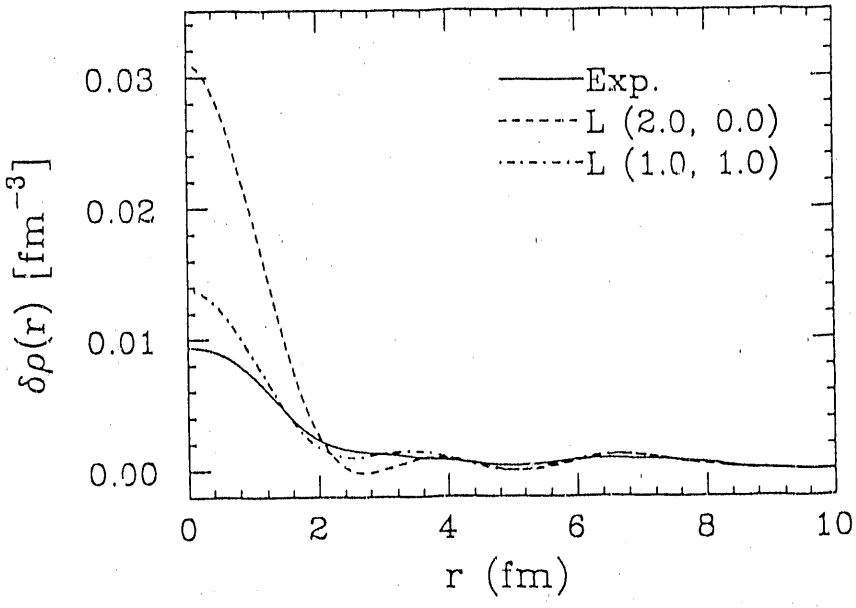

Fig. 4. Effects of fractional level occupancy on the ^{206}Pb−^{204}Hg charge density difference. The solid curve is the experimental result, the other curves are based on the linear version of QHD with (dashed) 2.0 protons removed from the 3s level and (dashed-dotted) 1.0 proton removed from the 3s level and 1.0 from the 2d level.

4. Meson Exchange Current Corrections to Magnetic Moments in Quantum Hadro-Dynamics T. M. Morse, C. E. Price and J. R. Shepard

In the early Quantum Hadro-Dynamics (QHD)[1] calculations of the magnetic moments of closed shell $\pm$ nuclei,[2,3] there was a significant disagreement with both experiment and the non-relativistic Schmidt moments. This disagreement was due to an enhancement of the convection current contribution to the magnetic moments, which was an indirect result of the reduced nucleon effective mass in QHD. Subsequent calculations[4] showed that problems with the isoscalar magnetic moments were an artifact of the treatment of the unpaired nucleon. The early calculations had assumed that the unpaired nucleon could be treated as a valence particle in the nearby closed shell system. This assumption effectively ignored the polarization of the closed shell core due to the presence (or absence) of the valence nucleon. McNeil *et al.*[4] showed that, by including this (isoscalar) core polarization in the random phase approximation, the enhancement of the convection current was eliminated and good agreement ($\leq 5\%$) with experiment was obtained for the isoscalar magnetic moments. Finally, in a fully self-consistent calculation that included the response of the valence particle to the polarization of the core, Furnstahl and Price[5] also obtained reasonable agreement with experiment ($\pm 10\%$) for the isovector magnetic moments. This last result is surprising since the model does not include the effects of the charged mesons and it is expected[5,6] that the meson exchange currents (MEC) due to charged mesons—especially pions—will have a significant effect on the isovector moments.

We have considered the corrections to the QHD magnetic moments due to a single charged pion exchange within the nucleus. The QHD-II Lagrangian[1] includes the interactions of nucleons with sigma, omega, rho and pi mesons (and Coulomb interactions); however, in many applications the pi meson does not contribute. For example, in uniform nuclear matter, spherical nuclei and even-even deformed nuclei the pion mean field vanishes. In the current calculation the pion can contribute in two ways. First, even if the pion mean field is zero, it is still possible to exchange virtual pions between two nuclei and the exchange of such charged pions give rise to the MEC corrections considered here. Secondly, in a completely self consistent calculation of an odd-A nucleus, the pion field does not vanish, so the pion can enter the calculation through the details of the mean-field basis.

The pion exchange contributions to the magnetic moment are described by the two Feynman diagrams shown in figure 1. These diagrams will have a non-zero contribution to the magnetic moments only if one of the nucleon lines corresponds to the valence nucleon (diagrams that do not involve the valence nucleon will cancel when the appropriate summation over core states is carried out).

Using the Feynman rules, it is simple to write down coordinate space expressions for the electro-magnetic currents corresponding to these two diagrams which

can be used to calculate the magnetic moments. We obtain

$$\Delta\mu_{seagull} = -\frac{2e\,{g_\pi}^2}{M}\int d^3r_1\; d^3r_2\;\bar{\psi}_p(\vec{r}_1)\left[\frac{\vec{r}_1\times\vec{\gamma}}{2}\right]_{10}\gamma^5\psi_n(\vec{r}_1) \\ \frac{1}{4\pi}\frac{e^{-m_\pi|\vec{r}_1-\vec{r}_2|}}{|\vec{r}_1-\vec{r}_2|}\bar{\psi}_n(\vec{r}_2)\frac{M^*(\vec{r}_2)}{M}\gamma^5\psi_p(\vec{r}_2) \tag{1}$$

and

$$\Delta\mu_{in-flight} = -2ie\,{g_\pi}^2\int d^3r_1\; d^3r_2\; d^3r\;\bar{\psi}_p(\vec{r}_1)\gamma_5\frac{M^*(\vec{r}_1)}{M}\psi_n(\vec{r}_1) \\ \frac{1}{4\pi}\frac{e^{-m_\pi|\vec{r}-\vec{r}_1|}}{|\vec{r}-\vec{r}_1|}\left[\frac{\vec{r}\times\overrightarrow{\partial}_r}{2}\right]_{10}\frac{1}{4\pi}\frac{e^{-m_\pi|\vec{r}_2-\vec{r}|}}{|\vec{r}_2-\vec{r}|}\bar{\psi}_n(\vec{r}_2)\gamma_5\frac{M^*(\vec{r}_2)}{M}\psi_p(\vec{r}_2) \tag{2}$$

where ψ is a nucleon wave function (p for proton, n for neutron), g_π and m_π are the pi-nucleon coupling and the pion mass, and M (M^*) is the nucleon mass (effective mass: M minus the sigma meson mean field). In deriving these expressions, we have assumed pseudo-vector coupling for the pion-nucleon interaction and have obtained the photon couplings by minimal substitution. We have evaluated these expressions in the closed shell ±1 systems near A=16 and A=40, using the spherical Hartree basis wave-functions (in QHD-II) appropriate to the nearby doubly closed shell nucleus. By doing so, we have neglected the effects of core polarization on the MEC corrections. This effect is expected to be small compared to the total magnetic moment. We have also neglected the effects of the pion mean-field in the odd-A system. Since this effect has not yet been studied and could alter not only MEC corrections but also the self-consistent QHD magnetic moments that we have used as our starting point, it is difficult to assess its importance. The additional corrections due to properly including the pion effects in the full odd-A wavefunctions will be the subject of a future investigation.

In Table I, we show the QHD pion exchange current correction to the magnetic moments of eight nuclei near A=16 and A=40. The self consistent QHD magnetic moments are from ref. 5 and are in qualitative agreement with the non-relativistic Schmidt moments and the experimental values. The MEC corrections (from this work) are relatively small and are of roughly the same magnitude as the typical discrepancy between the QHD moments and the experimental values. Unfortunately, the sign of the correction is opposite to that of the discrepancy.

In order to get a more accurate picture of these corrections, it is convenient to recast our results in terms of the isoscalar and isovector magnetic moments. These results are shown in Tables II and III. From Table II, it is clear that the QHD results are in rather close agreement with experiment and that the MEC corrections are negligible as is expected based on the isovector nature of the pion exchange (the isoscalar corrections would vanish only if we had ignored the differences between

	Schmidt	QHD	MEC	QHD+MEC	Expt
^{15}N	−0.264	−0.250	0.102	−0.148	−0.283
^{15}O	0.638	0.648	−0.101	0.547	0.719
^{17}O	−1.913	−2.03	0.162	−2.19	−1.894
^{17}F	4.793	4.89	−0.140	5.03	4.722
^{39}K	0.124	0.380	0.173	0.553	0.391
^{39}Ca	1.148	0.940	−0.174	0.766	1.022
^{41}Ca	−1.913	−2.20	0.277	−2.48	−1.595
^{41}Sc	5.793	6.08	−0.263	6.34	5.430

Table I. Magnetic moments of closed shell ±1 nuclei in nuclear magnetons.

A	QHD	MEC	QHD+MEC	Expt
15	0.199	0.001	0.200	0.218
17	1.43	-0.011	1.42	1.414
39	0.660	-0.001	0.659	0.706
41	1.94	-0.007	1.93	1.918

Table II. Valence (QHD) and one pion exchange corrections (MEC) to *isoscalar* magnetic moments.

the neutron and proton basis states which are due to Coulomb effects and the rho meson interaction). From Table III, it is clear that the discrepancy between the QHD isovector moments and the experimental values is somewhat larger than the corresponding discrepancy for the isoscalar moments, and that the meson exchange currents contribute a significant correction to these moments. For all of the systems that we studied (A=15, 17, 39 and 41), the MEC corrections significantly degrade the agreement of the QHD moments with experiment. This degradation is particularly large for the A=15 and 17 systems where the total magnetic moments are fairly small. These calculations could be improved by including the effects of core polarization on the MEC corrections, including pion contributions to the Hartree basis and by including additional isovector correction such as isobar current corrections and exchange current corrections due to other mesons.

A	QHD	MEC	QHD+MEC	Expt
15	−0.449	0.102	−0.347	−0.501
17	3.46	0.151	3.61	3.308
39	−0.280	0.174	−0.106	−0.316
41	4.14	0.270	4.41	3.512

Table III. Valence (QHD) and one pion exchange corrections (MEC) to *isovector* magnetic moments.

1. B. D. Serot and J. D. Walecka, Adv. in Nucl. Phys. **16**, 1 (1986).
2. L. D. Miller, Ann. Phys. **91**, 40 (1975).
3. B. D. Serot, Phys. Lett. **107B**, 263 (1981).
4. J. A. McNeil, R. D. Amado, C. J. Horowitz, M. Oka, J. R. Shepard and D. A. Sparrow, Phys. Rev. **C 34**, 746 (1986).
5. R. J. Furnstahl and C. E. Price, Phys. Rev. **C 40**, 1398 (1989)
6. R. J. Furnstahl and B. D. Serot, Nucl. Phys. **A468**, 539 (1987); J. R. Shepard, E. Rost, C. Y. Cheung and J. A. McNeil, Phys. Rev. **C37**, 1130 (1988); S. Ichii, W. Bentz and A. Arima, Nucl. Phys. **A487**, 493 (1988); R. J. Furnstahl, Phys. Rev. **C38**, 370 (1988).

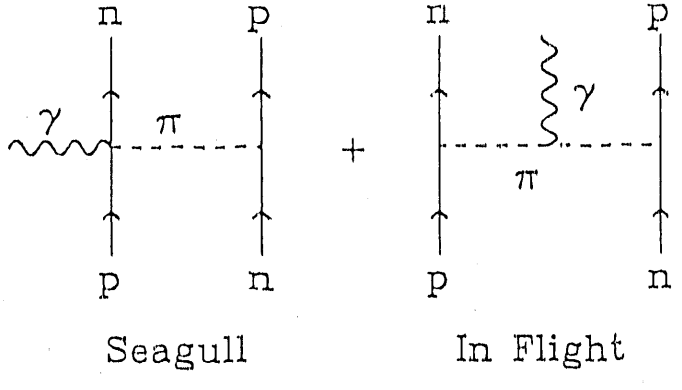

Fig. 1. The two Feynman diagrams (seagull and in-flight) which describe the pion exchange currents used to calculate the magnetic moment correction.

5. Analysis of the $0^+ \rightarrow 0^-$ Reaction at Intermediate Energies E. Rost and P.D. Kunz

The $0^+ \rightarrow 0^-$ transition by medium-energy proton inelastic scattering is a potentially rich source of new nuclear structure information. A general inelastic scattering reaction requires[1] three nuclear structure densities: the spin-independent longitudinal density, the spin-dependent transverse density and the spin-dependent longitudinal density. For a $0^+ \rightarrow 0^-$ transition only the last term is non-zero and hence can be studied in isolation from the other, generally larger, terms. The analysis usually involves a perturbation treatment with some form of distorted wave impulse approximation (DWIA) where only first-order effects are considered. Since such analyses[2] do not agree with the data, we were motivated to consider a generalization of the DWIA to include second-order terms.

Our analysis employs a simplified DWIA which uis based on a nucleon-nucleon t-matrix of the form

$$\check{t}_{NN}(q,Q) = A + B\vec{\sigma}_1 \cdot \vec{\sigma}_2 + C(\vec{\sigma}_1 + \vec{\sigma}_2) \cdot \hat{n} + D(\vec{\sigma}_1 \cdot \hat{q})(\vec{\sigma}_2 \cdot \hat{q}) + E(\vec{\sigma}_1 \cdot \hat{Q})(\vec{\sigma}_2 \cdot \hat{Q}), \quad (1)$$

where $\vec{q} = \vec{k}_i - \vec{k}_f$, $\vec{Q} = \vec{k}_i + \vec{k}_f$ and $\hat{n} = \hat{q} \times \hat{Q}$. Equation (1) is approximated by

$$\check{t}_{NN}(q,Q) \approx V^C(q) + V^\sigma(q)\vec{\sigma}_1 \cdot \vec{\sigma}_2. \quad (2)$$

The last term in Eq. (1) involving $\hat{Q}$ cannot be accomodated in a local t-matrix form and is ignored in this work. We have considered the fourth term, which is basically a tensor interaction, and can calculate the DWIA with it. However its effect is completely negligible for the $T = 0$ transitions in this work. The third term, a two-body spin-orbit term, is neglected here for calculational simplicity. We hope to repair this defect later. We note that explicit treatment of exchange is not included in this calculation—however some implicit effects of exchange are present since the experimental NN amplitudes are used.

The complex $V^C(q)$ and $V^\sigma(q)$ amplitudes are known from NN scattering and are fitted at each energy by a sum of Yukawa forms

$$V^j = 4\pi(\hbar c)^3 \sum_{i=1}^{5} \frac{V_i^j}{m_i c^2} \left[m_i^2 c^4 + \hbar^2 c^2 q^2\right]^{-1}, \quad (3)$$

for $j = C$ and σ and for isospins 0 and 1. Five masses (125, 350, 550, 900 and 1500 MeV) were found to give an adequate fit to the forward angle (less that 60°) NN "data". A local pseudo-potential may then be written

$$V = \eta \left[V^C(r) + V^\sigma(r) \vec{\sigma}_1 \cdot \vec{\sigma}_2 \right] \tag{4}$$

where

$$\eta = \frac{-4\pi(\hbar c)^2}{[m^2c^4 + Tmc^2/2]^{1/2}} \tag{5}$$

and T is the incident proton energy in the laboratory system. The configuration-space potentials are then

$$V^j(r) = \sum_{i=1}^{5} V_i^j \frac{\exp(-x_i)}{x_i}, \qquad x_i \equiv \frac{m_i c r}{\hbar} \tag{6}$$

for $j = C$ and σ.

Distorted waves are generated from optical potentials which have fitted elastic scattering data. At 400 MeV the optical parameters are taken form the work of Abdul-Jahil *et al.*[3]; at 180 MeV we adopt a "global" parametrization of Schwandt *et al.*[4].

The nuclear structure for the T=0, J^π=0$^-$ state of ^{16}O is believed to be very simple[5] and dominated by the $[p_{1/2}^{-1}s_{1/2}]$ configuration. We describe the single particle or hole states in terms of shell-model wavefunctions in a Woods-Saxon well of radius $1.25\times(16)^{1/3}$ fm and diffusivity 0.65 fm. A standard Thomas-form spin-orbit term of strength $\lambda = 25$ is used. Finally the depth of the well was adjusted so that the binding energies followed experimental energies [taken as the average of proton and neutron particle (or hole) energies.] These are E = (−20.72, −13.40, −2.37, −1.68) for the ($p_{3/2}$, $p_{1/2}$, $d_{5/2}$, $s_{1/2}$) orbitals. The results that follow are largly insensitive to the precise details of such choices.

Two reaction mechanisms are considered:
(1) A single-step excitation of the 0$^-$ final state;
(2) Two-step excitation via an intermediate $[p_{1/2}^{-1}\ d_{5/2}]_{3^-}$ state.

The 3$^-$ state is strongly excited in (p,p′) reactions and is readily calculated in the DWIA model. Figure 1 shows the cross section for (p,p′) at 180 MeV calculated with the impulse approximation where the calculated cross section has been multiplied by a factor of 2 to account for other configurations, or equivalently, some collectivity. This one-step excitation which proceeds through the V^C term in Eq. (2) is reasonably described in our simple model. For the de-excitation of the 3$^-$ state to the final 0$^-$ state, a spin-flip term is required, i.e. the transition involves L=2, S=1, J=3 and proceeds via the V^σ term of Eq. 2. We assume the same factor of two enhancement here as in the excitation process.

It is now possible to calculate a second-order DWIA, either alone (pure two-step) or in coherent combination with the one-step DWIA. In Figs. 2 and 3 we show the one-step, two-step, and coherent combination DWIA calculations for the excitation of the 0^- state by 180 MeV and 400 MeV protons, respectively. The calculated cross sections compare as well with the data as other, more sophisticated DWIA calculations.

The analyzing power results in Figs. 2 and 3 give the most significant result of this work. Although the two-step cross sections lie an order of magnitude below the one-step DWIA (and the data), the coherent sum of one- and two-step processes make for substantial effects in the calculated analyzing powers. The one-step calculation gives zero A_y values for a local interaction as may be rigorously shown[6] (our small values are due to a slight momentum difference between initial and final systems.) Earlier work[7] has attempted to explain the clearly non-zero experimental values with non-local (e.g., spin-orbit and exchange) terms in the one-step interaction. However the effect of two-step processes, although unimportant for the cross sections, should not be ignored in such analyses.

1. W.G.Love *et al.*, in *Proceedings of International Conference on Spin Excitations*, Telluride, CO, edited by F.Petrovich *et al.* (1982)
2. E.Rost in *Technical Progress Report, University of Colorado*, NPL1056, 80 (1989)
3. I.Abdul-Jalil and D.F.Jackson, J. Phys. **G5**, 1699 (1979)
4. P.Schwandt *et al.* Phys. Rev. **C26**, 55 (1982)
5. V.Gillet and N.Vinh Mau, Nucl. Phys **54**, 321 (1964)
6. S.S.M.Wong *et al.*, Phys. Lett. **140B** 299 (1984)
7. J.Piekarewicz, Phys. Rev. **C35**, 675 (1987)
8. J.J.Kelly *et al*, Phys. Rev. **C41**, 2504 (1990) and private communication
9. J.King, private communication

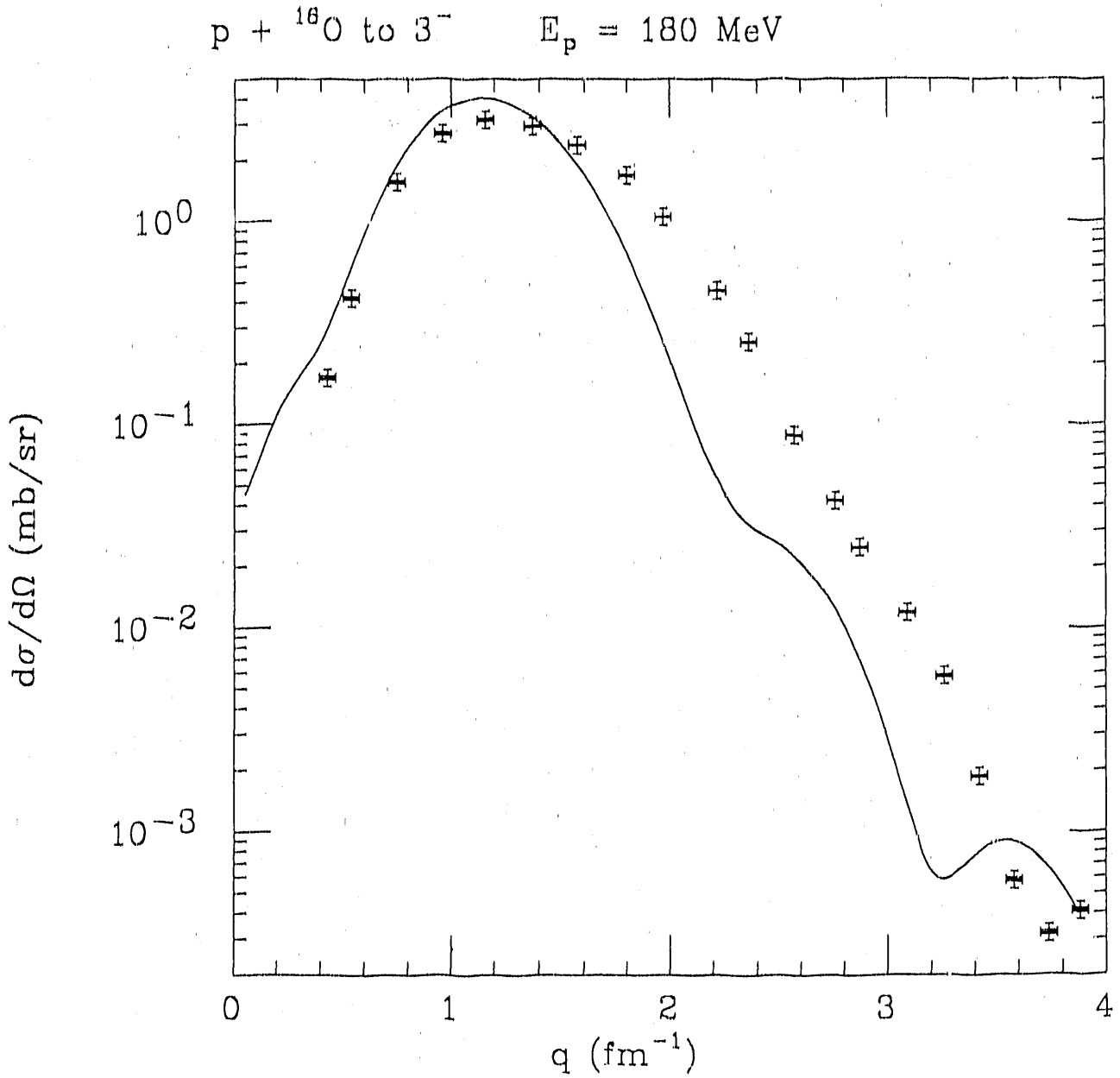

Fig. 1. Experimental and theoretical cross sections for the excitation of the 6.130 MeV 3^- level level of ^{16}O by 180 MeV protons. The data are taken from ref. 7. The theoretical curve is obtained from a simple first-order impulse as approximation described in the text and includes a renormalization factor of 2.

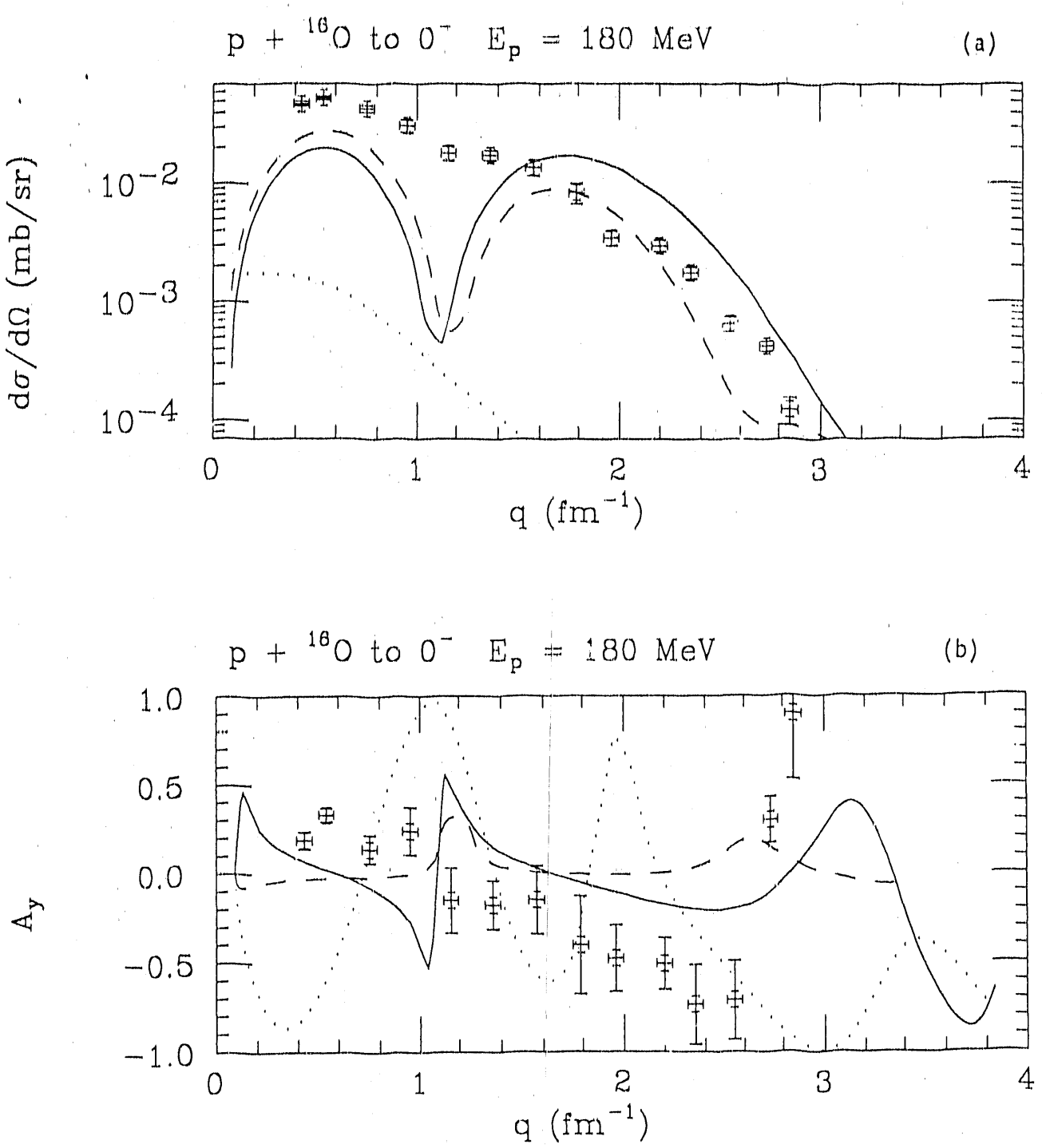

Fig. 2. Experimental and theoretical cross sections and analyzing powers for the excitation of the 10.957 MeV 0^- level of ^{16}O by 180 MeV protons. The data are taken from ref. 8. The dashed curve is obtained from a simple first-order impulse approximation described in the text. The dotted curve is obtained from a second-order DWIA via an intermediate 3^- state. The solid curve is obtained from both one- and two-step processes.

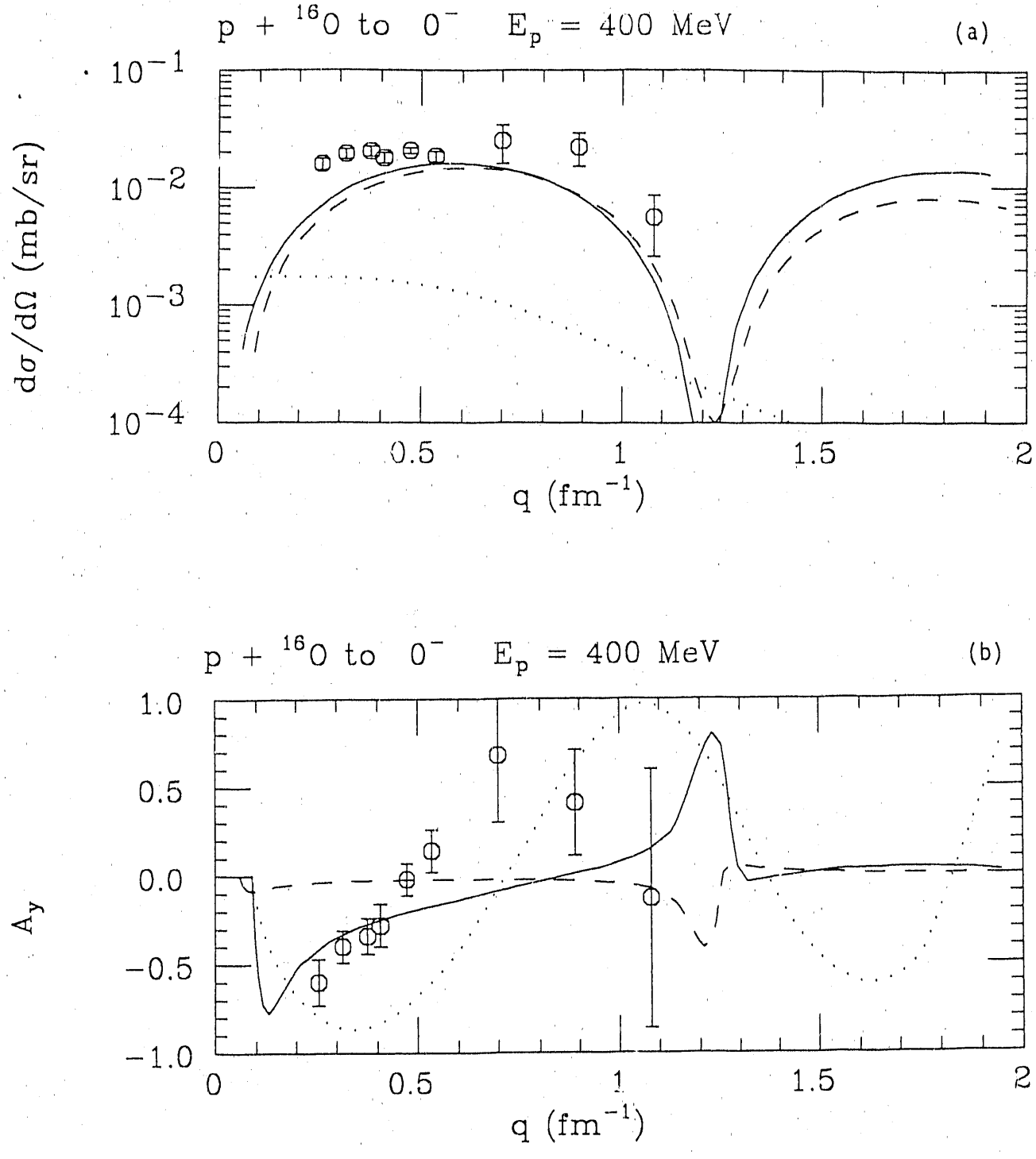

Fig. 3. Experimental and theoretical cross sections and analyzing powers for the excitation of the 10.957 MeV 0^- level of ^{16}O by 400 MeV protons. The data are taken from ref. 9. The dashed curve is obtained from a simple first-order impulse approximation described in the text. The dotted curve is obtained from a second-order DWIA via an intermediate 3^- state. The solid curve is obtained from both one- and two-step processes.

6. Contributions of Reaction Channels to the ^{6}Li(p,γ)^{7}Be Reaction

P.D.Kunz

At low bombarding energies the strength of the ^{6}Li(p,γ)^{7}Be reaction to the ground and first excited state is larger by a factor of two than that calculated from a simple direct capture model[1]. In this model an effective potential model is constructed for the interaction. The γ-ray transition is dominated by the electric dipole transition from the continuum s states to a p state in the final nucleus. The spin 1/2 channel gives the main contribution to the cross section because of the small amplitude of the spin 3/2 component in ^{7}Be. The potential model is fitted separately to the s wave scattering lengths for the spin 1/2 and spin 3/2 ^{6}Li + p channels. The scattering length for the spin 1/2 system is large and positive and its potential supports a bound state of a few MeV binding energy. However the experimental evidence for such a $1/2^+$ level in ^{7}Be is lacking. In addition the fitted potential must contain an imaginary part to account for the breakup reaction ^{6}Li(p,^{3}He)^{4}He. The results of calculations with this simple model describe the energy dependence of the (p,γ) cross section but fail to fit the magnitude of the data.

An open ^{3}He + ^{4}He channel can give rise to a large effect but a simple local potential model with an imaginary component may not describe properly the removal of flux from the initial channel. Therefore we consider a self consistent model for the reaction which takes into account *both* capture and breakup processes. The latter process can be considered to be a deuteron exchange process[2] between the proton and ^{6}Li or, equivalently, a ^{6}Li(p,^{3}He)^{4}He reaction. If the ^{3}He + ^{4}He channel is coupled back into the initial channel then the effects of the absorption can treated in a more natural way than by relying on an imaginary term in the potential. The reaction is depicted as

$$^6\mathrm{Li} + \mathrm{p} \leftrightarrow ^3\mathrm{He} + ^4\mathrm{He}$$

$$^6\mathrm{Li} + \mathrm{p} \rightarrow ^7\mathrm{Be} + \gamma$$

in a coupled channels formulation. The equations can be easily formulated and solved using the coupled channel code CHUCK3. In addition a contribution to the gamma ray transition also results from the breakup channel

$$^3\mathrm{He} + ^4\mathrm{He} \rightarrow ^7\mathrm{Be} + \gamma.$$

This component is coherent with the direct capture process and has no extra suppression from the Coulomb barrier since the channel has an energy of about 4 MeV.

Preliminary calculations have studied the effect of the explicit inclusion of the breakup reaction channel. The parameters of the model are adjusted to reproduce the known breakup cross section. The most sensitive parameter is the strength of the channel coupling. The fit to the breakup data gives the scattering lengths for the two spin channels within 10% and closer agreement may be obtained by adjusting the range parameters in the two-nucleon transfer form factor. This agreement involves *no* additional potential terms in the initial $p + {}^6\mathrm{Li}$ channel. A preliminary calculation also shows better agreement with the magnitude of the capture cross section.

1. F.C. Barker, Austr. J. Phys. **33**, 159 (1980)
2. H. Weigmann and P. Manakos, Zeitschrift für Physik, **A289**, 383 (1979)

7. Deformed Chiral Nucleons C. E. Price and J. R. Shepard

The fundamental field theory of the strong interaction, QCD, has not yet evolved to a form which makes possible quantitative, first-principle calculations of low-energy hadronic properties. Nevertheless, there is general agreement that, when such calculations are done, they will be consistent with the ideas of quark confinement and hidden chiral symmetry. Much effort has been expended to develop phenomenological field theories which are at once calculationally tractable and also to some degree compatible with QCD. A familiar example is that of the Skyrme model[1] which can be interpreted as the large N_c limit of low-energy QCD[2] and whose topological solitons possess both the properties of absolute confinement and hidden chiral symmetry. It is both the strength and weakness of the Skyrme models that they make no explicit reference to quarks. Non-topological soliton (or hybrid) models[3] have been put forward as alternatives which include quark degrees of freedom throughout. These models still possess hidden chiral symmetry but the quarks are not absolutely confined. This latter shortcoming, it may be argued, should not be distressing provided the binding energy of the quarks in hadrons is large on the scale set by our definition of the "low-energy" nadronic properties we seek to describe. In any case, such hybrid models, typically based on elaborations of the Lagrangian of the σ-model,[4] can provide very economical descriptions of, *e.g.*, the N-Δ system. For example, the calculations of Birse and Banerjee[3] and reproduce with reasonable accuracy nucleon properties such as rest mass, magnetic moments, rms radii, g_A and $g_{\pi NN}$ with essentially two free parameters, namely the coupling constant g for the interaction between the quarks and the chiral field (or equivalently, the effective quark mass) and m_σ, the mass of the scalar meson. These and virtually all other hybrid model calculations employ the "hedgehog" ansatz. This amounts to assuming that the pion field has the form $\vec{\pi} = \pi\hat{r}$ and then calculating an intrinsic state in which isospin $\vec{I}$ and angular momentum $\vec{J}$ are coupled to yield a state for which the "grand spin" $\vec{K} = \vec{I} + \vec{J}$ is a good quantum number. Since the matrix elements of the quark spin and isospin operators are readily evaluated for such states, significant calculational simplifications are achieved. More significantly, it has been shown that the hedgehog is a local minimum of energy at least with respect to some restricted variation. However, it is also true that the hedgehog is an unphysical object and physical states with well defined $\vec{I}$ and $\vec{J}$ must be projected from it much as, in the standard treatment of deformed nuclei, states of "good" angular momentum must be projected from a deformed intrinsic state.

With these difficulties in mind, we have developed an alternative to the hedgehog model which utilizes techniques employed in calculations of deformed nuclear ground states in the framework of quantum hadrodynamics (QHD[6]), a relativistic quantum field theory of nuclear structure. We begin with the standard Lagrangian of the non-linear σ model (see, *e.g.*, Reference 3) including a chiral symmetry breaking term that generates a quark mass (through the non-zero vacuum expectation value of the σ field). Our method diverges from the hedgehog approach in that we assume our three-quark wave functions have spin-isospin structure corresponding to the usual SU(6) wave function for a spin-up proton. Our solutions therefore

possess the proper spin and isospin *projections* by construction. Furthermore, if the single quark wave functions were degenerate, our nucleon would have the correct *total* isospin, as well. If we assume the quarks are in s-states, the equation of motion for the neutral pion field implies $\pi_0 \propto \cos\theta$ where $\theta = \hat{r} \cdot \hat{z}$ is the usual polar angle (charged pion mean fields are excluded in this model). The pi–quark interaction can then couple, *e.g.*, the lower component of an $s_{1/2}$ quark wave function to the upper component of a $d_{3/2}$ wave function. This means that the neutral pion field can induce deformations in our mean-field solution for the nucleon. We allow for this possibility in our calculations and find single quark wave functions whose energies are split by their interaction with the π_0 field which changes sign upon flip of either spin or isospin. However, this splitting is not large and we have estimated isospin projection by itself to be a 5 to 10% effect at most. If we ignore this small violation of isospin symmetry, we conclude that we have calculated an object intermediate between the hedgehog intrinsic state which is a mixture of various spins *and* isospins and the physical state which has unique values of spin and isospin. Of course we still face the task of projecting physical states of good total angular momentum as is done in standard treatments of deformed nuclei.

In Table 1, we compare the results of our calculation of nucleon properties with those of Birse and Banerjee[3] and with experiment. Our (Birse and Banerjee's) calculations use best-fit parameters $m_q = 1200$ (500) MeV and $m_\sigma = 600$ (1200) MeV. We show two sets of our results, one designated as "spherical" which includes only $s_{1/2}$ quark wave functions and another labelled "deformed" which allows up to $g_{7/2}$ admixtures. In the deformed (spherical) calculation, the σ' field has $L = 0$ and 2 ($L = 0$) multipoles while the π_0 field has $L = 1$ and 3 ($L = 1$). We have determined empirically that higher multipoles in either the quark wave functions or the meson fields are of negligible importance. The major difference between the spherical and deformed calculations is due to the presence of the $d_{3/2}$ components in the quark wave functions. The amount of deformation may thus be quantified in terms of the amplitude of the $d_{3/2}$ component of the quark wave functions and is found to be 14% for the deformed calculations presented in Table 1. Another measure of the departure from sphericity is the standard deformation parameter which is $\beta_2 = -0.26$ (for the quark scalar density) in the present case indicating an oblate deformation. As the numbers in the table show, this modest deformation has profound effects on the nucleon properties. Deformation reduces the $u_\uparrow/d_\downarrow$ versus $u_\downarrow/d_\downarrow$ splitting by 690 MeV (to only 224 MeV), increases the total mass by 353 MeV, changes the magnetic moments by about 45% and reduces g_A and $g_{\pi NN}$ by nearly a factor of three putting them in essentially exact agreement with experiment! (Note that g_A and $g_{\pi NN}$ are constrained to be proportional by the Goldberger-Trieman relation, $g_A M = g_{\pi NN} F_\pi$, which is realized at the level of $g_A M / g_{\pi NN} F_\pi = 0.961$ (0.785) for our deformed (spherical) calculation.) Perhaps the most striking difference between our calculations and those for the hedgehog is that our pion field (and hence, its contribution to the nucleon mass) is much smaller than that of the hedgehog. The weakness of our π_0 field is closely connected with the deformation of the quark wave functions. Recall that the π_0 field has a $\cos\theta$ spatial dependence and is therefore strongest at the nucleon "poles" and vanishes at the "equator." Though the interaction of the quarks with this field is attractive

for $u_\uparrow$ and $d_\downarrow$ and repulsive otherwise, the total nucleon energy is minimized by minimizing the π_0-quark interaction. In the present model, this is accomplished by an oblate deformation which effectively concentrates the quarks in the "equatorial" region. In turn, this weakens the π_0 source and finally the overall π_0 field strength.

Except for the mass which is subject to sizeable reductions due to center-of-mass corrections, the deformed calculations of the properties of the nucleon are in excellent agreement with experiment. Furthermore, no parameter combination could be found which gave even *remotely* comparable agreement for the spherical calculation. Deformation is evidently a crucial degree of freedom in this model! Again except for the mass, our deformed calculation gives a description of the nucleon which in almost every instance is comparable or superior to that of the hedgehog. The values of g_A and $g_{\pi NN}$ in particular are much better accounted for by the deformed calculation. Only our value for the σ-nucleus commutator,[3,8,9] $\sigma_{\pi N}$, is in substantial disagreement with experiment[9] and in fact is somewhat worse than the hedgehog result. Regardless of how the two models fare in comparisons with data, perhaps the most interesting result is that they require such different inputs to describe the nucleon. In fact, our calculations do not generate a bound system when we use the Birse and Banerjee best-fit parameters. These differences in values of m_q and m_σ are difficult to understand and provide a strong incentive to understand the formal relation between deformed and hedgehog solutions. This will be the subject of a future publication.

While differences between best-fit parameters for the deformed and the hedgehog solutions are noteworthy in their own right, the specific values we find for m_q and m_σ have their own interesting implications. We mentioned above that hybrid models such as ours do not give absolute confinement. The energy scale on which the quarks are *effectively* confined is given by the quark binding energy. In the Birse and Banerjee hedgehog, as shown in Table 1, this energy is ~470 MeV. By taking the average of our quark binding energies with weights fixed by the SU(6) wave functions, our quark binding energy is found to be 900 MeV (1125 MeV) for the deformed (spherical) calculation. Thus our quarks are substantially better confined than those of the hedgehog.

Assessing which σ-mass is most physical is a challenging problem principally because the σ is not physical. However, most workers in this field have their own prejudices. Birse and Banerjee, for example, seem happy with their value of 1200 MeV because it is consistent with "that observed from πN scattering and the observed $\epsilon(1300)$ resonance." Our prejudices are somewhat different. There have long been suggestions of a very broad σ-resonance at about 600 MeV. Notwithstanding its glaring absence from the Particle Properties Data Booklet, this σ-meson has played a prominent role in nuclear physics. In fact many of the arguments in favor of using this mythical σ-meson have the same flavor as those used to justify the Skyrme model and its offspring. Its presence is central to the QHD models[6] mentioned above where it provides the strong isoscalar attraction which, when balanced by the isoscalar repulsion from the ω, yields an economical relativistic description of many aspects of nuclear dynamics. The relationship - if any - between our σ component of the chiral field and the σ of nuclear physics has not been established. However, the fact that their masses are compatible in our model gives at least some encouragement to pursue this question.

We have computed nucleon properties using a hybrid chiral model. Instead of employing the hedgehog ansatz, we have computed a mean field solution with well defined spin and isospin projections. Our model allows for spatial deformation of the nucleon. Even though this deformation is modest, it is crucial in bringing about agreement with experiment, especially for quantities like magnetic moments and g_A. Our best fit involves only two free parameters and is generally superior to that of the hedgehog with very different values for the parameters. Our solution also differs from the hedgehog by having a much weaker pion field. Elucidating the formal connection between our deformed solution and the hedgehog is a high priority for the future as are treatment of sea quark effects and the study of a possible connection between the chiral field of the nucleon and the σ-field of, *e.g.*, QHD. Of highest priority is the study of the effects of full spin *and* isospin projection. The former especially may lead to major modifications of the unprojected results presented here. Such projected calculations are in progress.

1. T.H.R. Skyrme, Proc. R. Soc. London **A260**, 127 (1961); Nuclear Physics **31**, 556 (1962); J. Math. Phys. **12**, 1735 (1971)
2. E. Witten, Nuclear Physics **B223**, 422 (1983); Nuclear Physics **B223**, 433 (1983); G. Holzwarth and B. Schwesinger, Reports on Progress in Physics **49**, 825 (1986)
3. M.C. Birse and M.K. Bannerjee, Physics Letters **136B**, 284 (1984); Physical Review **D31**, 118 (1985)
4. M. Gell-Mann and M. Levy, Nuovo Cimento **16**, 705 (1960)
5. K. Goeke, J.N. Urbano, M. Fiolhais and M. Harvey, Physics Letters **164B**, 249 (1985)
6. R.J. Furnstahl and C.E. Price, Physical Review **C40**, 1398 (1989)
7. B.D. Serot and J.D. Walecka, Advances in Nuclear Physics, **16**, 1 (1986)
8. W. Bronioski and M. K. Banerjee, Physics Letters **158B**, 335 (1985)
9. J. Gasser, H. Leutwyler, M.P. Locher and M.E. Sainio, Physics Letters **213B**, 85 (1988)

	Spherical	Deformed	Hedgehog	Experiment
$(E-m)_1$	−1328 MeV	−950 MeV	−469.5	—
$(E-m)_2$	−413 MeV	−724 MeV	−469.5	—
M_N	1149/693 MeV	1502/1158 MeV	1116 MeV	939/1086 MeV
$\langle r^2\rangle_q^{1/2}$	0.68 fm	0.71 fm	—	—
$\langle r^2\rangle_{ch,p}^{1/2}$	0.66 fm	0.70 fm	—	0.85 fm
μ_p	1.79 nm	2.85 nm	2.87 nm	2.79 nm
μ_n	−1.54 nm	−2.00 nm	−2.29 nm	−1.91 nm
g_A	3.63	1.255	1.86	1.25
$g_{\pi NN}\ m_\pi/2M$	3.47	0.98	1.53	1.00
$\sigma_{\pi N}$	115 MeV	118 MeV	92.5 MeV	59 MeV

Table 1. Experimental and calculated nucleon properties. The spherical and deformed calculations refer to the present work with m_q=1200 MeV and m_σ=600 MeV. The hedgehog calculations are from Reference 3 and assume m_q=500 MeV and m_σ=1200 MeV. The quantity $(E-m)_1$ is the binding energy for the $u_\uparrow$ and $d_\downarrow$ single quark wave functions while $(E-m)_2$ refers to the other pair. RMS radii for the vector quark density and the proton charge density are quoted along with proton and neutron magnetic moments, the axial vector coupling constant and the πNN coupling constant. The σ-nucleus commutator $\sigma_{\pi N}$ is discussed in, *e.g.*, References 3 and 8. Both the nucleon mass and the average N-Δ mass appear for the experimental value of M_N. Values with and without the center-of-mass correction are displayed for our spherical and deformed calculations.

8. Vacuum Polarization in a Finite System T.C. Ferree and J.R. Shepard

The nucleus can be viewed as a many-body system of nucleons interacting via the exchange of virtual mesons, and the Walecka model (QHD-I) has been very successful in describing the nuclear structure of closed-shell systems from this point of view.[1] The nucleons are taken to be spin-$\frac{1}{2}$ point particles described by the Dirac equation, coupled to both intermediate-range attractive and short-range repulsive meson fields. It is well known that the Dirac equation predicts the existence of negative energy particles which cannot be ignored in a consistent treatment of the problem. In particular, virtual particle-antiparticle pair production, or vacuum polarization, in the meson propagators can significantly influence nuclear structure.

Ground state calculations in QHD-I usually employ the self-consistent Hartree approximation, which assumes that each nucleon interacts with the nucleus through background classical meson fields. So far, vacuum polarization has either been ignored entirely (MFT) or included in various Thomas-Fermi approximations (LDA and DE). It is possible, however, to include the effects of vacuum polarization exactly within this model; this is known as the Exact Relativistic Hartree Approximation (ERHA).

The model QHD-I is defined by a Lagrangian density in which the nucleons interact via the exchange of a repulsive ω-meson vector field V^μ, and an attractive σ-meson scalar field ϕ.

$$\begin{aligned}\mathcal{L} =& \bar{\psi}[\gamma_\mu(i\partial^\mu - g_v V^\mu) - (m - g_s\phi)]\psi + \frac{1}{2}(\partial_\mu\phi\partial^\mu\phi - m_s^2\phi^2) \\ & - \frac{1}{2}(\frac{1}{2}F_{\mu\nu}F^{\mu\nu} - m_v^2 V^\mu V_\mu) + \mathcal{L}_{ct}\end{aligned} \tag{1}$$

Both the vector and scalar mesons are isoscalar particles. Also included are counterterms which allow the renormalization of divergences arising when the infinite number of negative energy nucleon states is not ignored. The coupling parameters g_s and g_v are determined by solving the infinite nuclear matter problem and adjusting them until the nucleon density and the Fermi momentum equal those given by experimental data. Since the σ-meson is ficticious, m_s is entirely a free parameter in this model. Note that in the rest frame of the ground state nucleus, $V^\mu(x) = \delta^\mu_0\ V^0(x)$.

As a model calculation, we consider the finite problem in one spatial dimension, imposing periodic boundary conditions. The period is chosen to be large (20-30 fm) compared to the size of the nucleus. Parity is the analog of angular momentum in one dimension, and both nucleon and meson fields are parity eigenfunctions in this case. Also, there can be no intrinsic spin in one dimension since there is no way to satisfy the angular momentum commutation relations.

We have solved the MFT problem in one spatial dimension for N=Z nuclei with 1 through 4 closed shells. In this approach, one begins with a reasonable guess for the meson fields and numerically calculates the nucleon eigenstates. The occupied

states then become sources for the meson fields. In MFT, only the positive energy states are considered to be occupied. An iterative method allows the solutions to evolve to a self-consistent solution which no longer depends on the initial guess made for the meson fields. Figure 1 shows the results in the case of three closed shells, which is the one dimensional analog of ^{40}Ca. Based on the self-consistent meson fields one can construct a basis of nucleon eigenstates, the orthogonality and completeness of which has been verified numerically.

The simplest approximation which includes vacuum polarization effects is the Local Density Approximation (LDA).[2] Here the source of the scalar field is taken to have a negative energy contribution equal to that in the infinite system, but where the interacting nucleon mass $m^* = m - g_s\phi$ has spatial dependence through the scalar field $\phi(x)$.

$$\rho_s^{(-)}(x) = \frac{\lambda}{\pi}[m - m^* + m^* ln\frac{m^*}{m}] \tag{2}$$

By adjusting m_s, this solution may be forced to have the same rms size as the MFT solution. A qualitative difference, however, is that in the LDA solution the scalar source is slightly larger than the vector source, as seen in Figure 2. This result is also unlike the LDA result in three dimensions, where vacuum polarization *reduces* the strength of the scalar source. The Derivative Expansion (DE) is an improved Thomas-Fermi approximation which includes the derivatives of the meson fields, but still assumes that the nucleon wavefunctions behave locally as plane waves.[3] Work is currently in progress to investigate a self-consistent application of the DE to the one dimensional finite system.

The most obvious method of handling vacuum polarization exactly makes use of the spectral green function.

$$G^{ij}(x, y; w) = \sum_\alpha \frac{\psi_\alpha^i(x)\bar{\psi}_\alpha^j(y)}{\omega - \omega_\alpha + i\eta_\alpha} \tag{3}$$

Here the meson field sources include contributions from the infinite number of negative energy nucleon states known as the Dirac sea. Periodic boundary conditions discretize the unbound continuum states, so that each state may be labeled according to nodes and parity and solved for numerically. The Dirac sea contributions are rendered finite by choosing counterterms in such a way that the meson sources vanish in the vacuum. Summing explicitly over an infinite number of negative energy states poses a numerical problem, but after renormalization the results converge once one has gone "deep enough" into the Dirac sea.

Another exact method makes use of the nonspectral green function.[4]

$$G^{ij}(x, y; w) = \sum_\pi [\psi_u^i(x)\bar{\psi}_v^j(y)\theta(y - x) + \psi_v^i(x)\bar{\psi}_u^j(y)\theta(x - y)] \tag{4}$$

This method has been applied to a finite system [5], but never before in a self-consistent manner including both vector and scalar mesons.

The spectral and nonspectral green functions are *exactly* equivalent, which provides an excellent verification of these calculations. The nonspectral approach, however, will have advantages later when normal mode (RPA) excitations of the finite system are investigated. Work is well in progress using both the spectral and nonspectral methods to calculate exactly vacuum polarization effects in the ground state system.

1) B.D. Serot and J.D. Walecka, Adv. Nucl. Phys. **16**, 35 (1986)
2) C.J. Horowitz and B.D. Serot, Phys. Lett. 140B, 181 (1984)
3) R.J. Perry, Phys. Lett. B **182**, 269 (1986)
4) J.R. Shepard, E. Rost, C.Y. Cheung, J.A. McNeil, Phys. Rev. C **37**, 1130, (1988)
5) P.G. Blunden, Phys. Rev. C 41, 1851, (1990)

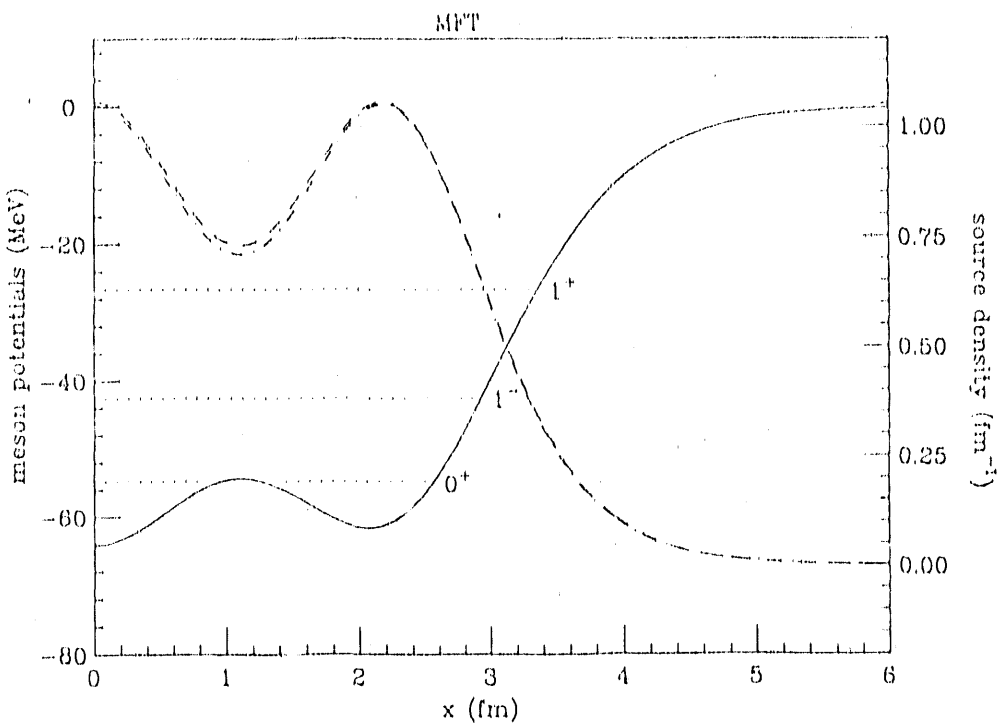

Fig. 1. Self-consistent MFT solution. The solid curve is the sum of vector and scalar meson potentials, with nucleon eigenenergies indicated by dotted curves. The dashed curve is the vector source density equal to the nucleon particle density. The dot-dashed curve is the scalar source density.

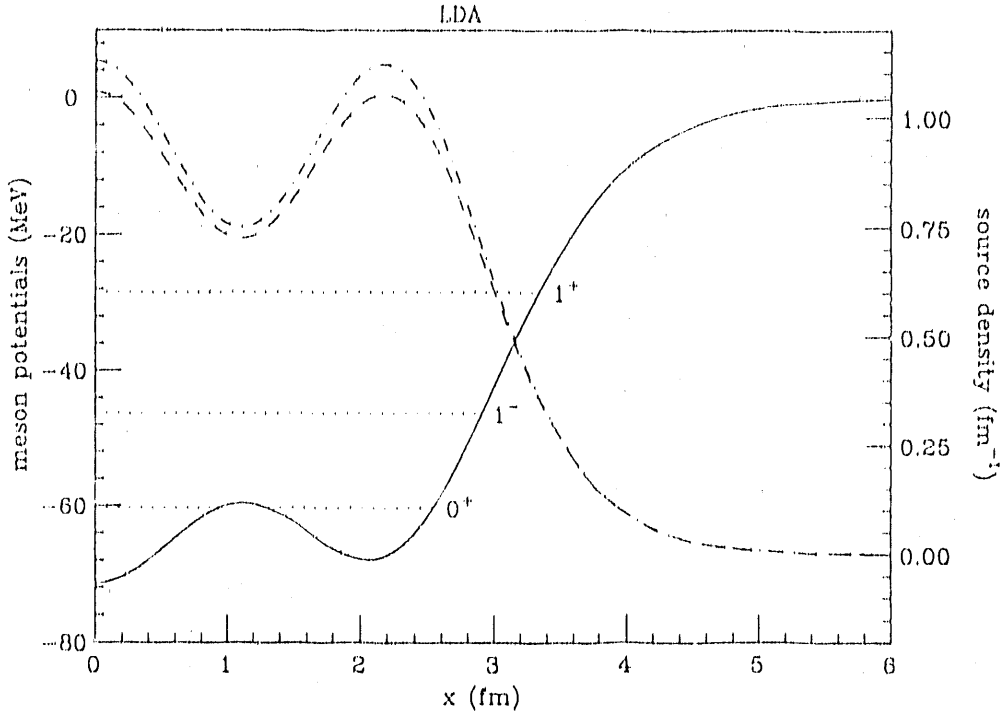

Fig. 2. Self-consistent LDA solution. The curves represent the same quantities as in Figure 1.

9. Second Order Processes in the $(e, e'd)$ Reaction P.D. Kunz and H.P. Blok (NIKHEF)

The $(e, e'd)$ knockout reaction leaving the deuteron in its ground state allows one to study certain aspects of nucleon-nucleon correlations in nuclei. Recent high quality data from NIKHEF allows the opportunity for the extraction of these features of nuclear structure. The deuteron knockout differs from the proton knockout reaction in that the outgoing particle has structure and its decription is more complicated. In order to reliably extract the structure information the reaction mechanism must be understood.

By neglecting the Coulomb distortions for the electron one can use plane wave states and the transition amplitude in first order Born approximation may be modelled as deuteron pickup by a light fictitious particle of momentum q,

$$T_{if} = f_e(\theta) \left\langle \chi_0^-(\mathbf{R}) \,|\, f_0(\mathbf{R}) \,|\, e^{i\mathbf{q}\cdot\mathbf{R}} \right\rangle. \qquad (1)$$

Here $f_e(\theta)$ is the Coulomb amplitude, $\chi_0^-(\mathbf{R})$ is a distorted wave for the deuteron center of mass motion and $\mathbf{q}$,$\mathbf{k}_i$ are the momentum transfer and inital momentum of the electron respectively. The form factor f_0 is an integral of the deuteron ground state wave function $\phi_0(\mathbf{r})$ with the overlap between the initial and final target states $u(\mathbf{r}_p, \mathbf{r}_n)$.

$$f_0(\mathbf{R}) = \left\langle \phi_0(\mathbf{r}) \,|\, e^{i\mathbf{k}_i\cdot\mathbf{r}} u(\mathbf{r}_p, \mathbf{r}_n) \right\rangle$$

This amplitude for the knockout reaction has the same general structure as the matrix element for the two nucleon transfer reactions (TNT) such as $(p, {}^3He)$.

It is well known that the direct first order term does not adequately describe[1] the TNT reactions and that second order processes such as sequential transfer are important. The derivation of the second order processes may be formulated via two different methods of expansion of the exact transition amplitude. In the first of these the reaction may proceed by the knockout of a deuteron to one of its continuum states followed by the transition to its ground state via the interaction of the deuteron with the nuclear field before escaping. In the second method the ejection of the deuteron may be considered as the knockout of a proton with the subsequent pickup of a neutron by the outgoing proton. If the corrections to all order were used in each of the two methods, the resulting cross sections would be identical. However, truncations must be made in order to allow computation of the results and to determine which method gives a better description of the reaction.

In the first method (the continuum model), the transition amplitude can be expressed by generalizing the outgoing deuteron wave for the ground state in (1) to include the continuum channels for the deuteron internal motion. The amplitude

becomes

$$T_{if} = f_c(\theta) \sum_n \langle \chi_n^-(\mathbf{R}) \,|\, f_n(\mathbf{R}) \,|\, e^{i\mathbf{q}\cdot\mathbf{R}} \rangle, \tag{2}$$

where

$$f_n(\mathbf{R}) = \langle \phi_n(\mathbf{r}) \,|\, e^{i\mathbf{k}_1\cdot\mathbf{r}} u(\mathbf{r}_p, \mathbf{r}_n) \rangle.$$

Here, the sum on n denotes summation over the bound and integration over the continuum set of deuteron states. The summation is truncated to include only the s states and the distorted waves $\chi_n^-(\mathbf{R})$ may be solved for by a suitable discretization[2,3] of the continuum. A preliminary calculation of this process in a schematic model is shown in Fig. 1 as a function of the number of continuum states included in the calculation. The calculation converges rather rapidly as the number of channels is increased and the main effect is to renormalize the cross section by factors of 2-3 over the ground state only case (one channel).

In the sequential knockout method the second order term can be transformed by a post-prior interchange of the pickup interaction giving rise to a correction term. This term can be shown[1] to exactly cancel the first order knockout term leaving only the sequential knockout for the amplitude through second order,

$$\begin{aligned} T_{fi} = f_c(\theta) \langle \chi_0^-(\mathbf{R}) \phi_0(\mathbf{r}) \,|\, v_{np}(\mathbf{r}_{np}) u_n(\mathbf{r}_n) \\ \times \frac{1}{E_p^- - K_p - U_p} u_p(\mathbf{r}_p) \,|\, e^{i\mathbf{q}\cdot\mathbf{r}_p} \rangle, \end{aligned} \tag{3}$$

where the u_p and u_n are the form factors for the knockout and pickup vertices in the reaction.

Although this amplitude is of second order it may be calculated by recasting it into a solution of a set of coupled equations. In order to facilitate the solution of these equations a first order range correction to a zero range approximation is usually made for the interaction v_{np}. The result of this calculation is shown in Fig. 2 along with the 7 channel result from Fig. 1 for comparison. As seen in the figure the sequential knockout cross section is almost an order of magnitude larger at forward angles than the continuum case. While the range correction for a (p,d) reaction on the energy-shell is usually small, the propagator for the intermediate proton state gives rise to a large off shell component to the range correction[4]. Preliminary calculations including both of the off-shell terms to first order indicate that this correction is as large as the main term. This is in contrast to the (p,t) reaction[5] where the range correction is rather small. Since the off-shell correction is large, a more exact method of evaluating the transition amplitude using full finite range techniques must be employed.

In Eq. 3 the knockout vertex is local and the intermediate proton wave may be derived from a set of equations with a source term,

$$(E_p - K_p - U_p)\chi_p^+(\mathbf{r_p}) = u_p(\mathbf{r_p})e^{i\mathbf{q}\cdot\mathbf{r_p}}, \tag{4}$$

where $\chi_p^+(\mathbf{r_p})$ has the boundary conditions of outgoing waves only. The resulting transition amplitude is

$$T_{fi} = f_c(\theta)\left\langle \chi_0^-(\mathbf{R})\phi_0(\mathbf{r}) \,|\, v_{np}(\mathbf{r_{np}})u_n(\mathbf{r_n}) \,|\, \chi_p^+(\mathbf{r_p})\right\rangle. \tag{5}$$

The pickup vertex must be treated in finite range with a readily available finite range distorted wave computer program such as DWUCK5[6]. Work on the conversion of the finite range program to allow for the calculation of the transition amplitude without the zero range approximation is in progress.

1. P.D. Kunz and E. Rost, Phys. Lett. **47B**, 136 (1973), J. Bang and S. Wollesen, Phys. Lett. **33B**, 396 (1970)
2. J.P. Farrell Jr., C.M. Vincent and N. Austern, Ann. of Phys. **96**, 333 (1976)
3. N. Austern, C.M. Vincent and J.P. Farrell Jr., Ann. of Phys. **114**, 93 (1978)
4. P.D. Kunz and L.A. Charlton, Phys. Lett. **72B**, 7 (1977)
5. H. Wienke H.P. Blok and J. Blok, Phys. Lett. **164B**, 7 (1985)
6. P.D. Kunz, DWUCK5 computer program, unpublished

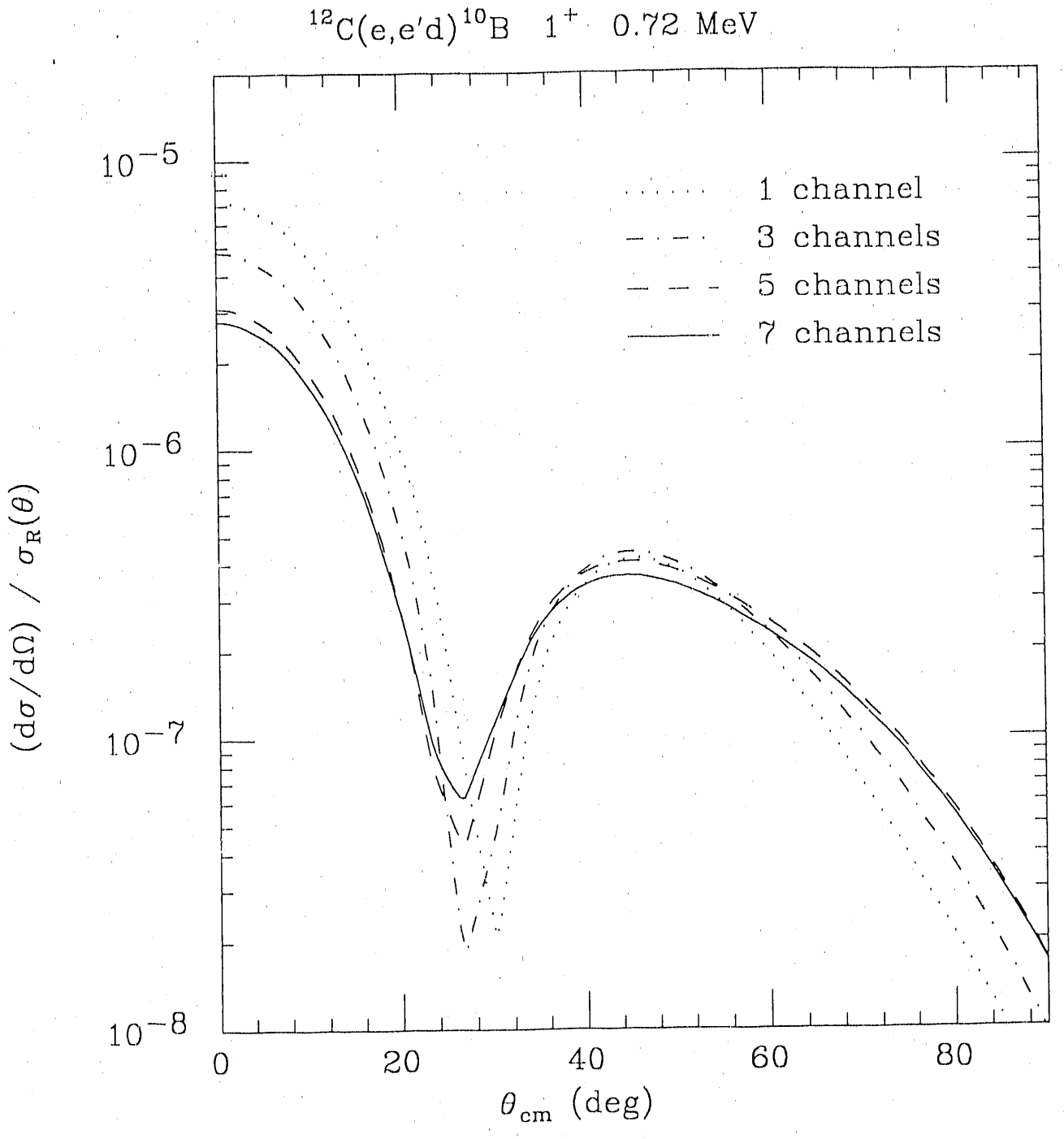

Fig. 1. The ratio of the cross section to Rutherford for the continuum model as a function of the number of channels included. The ground state case only is the 1 channel calculation.

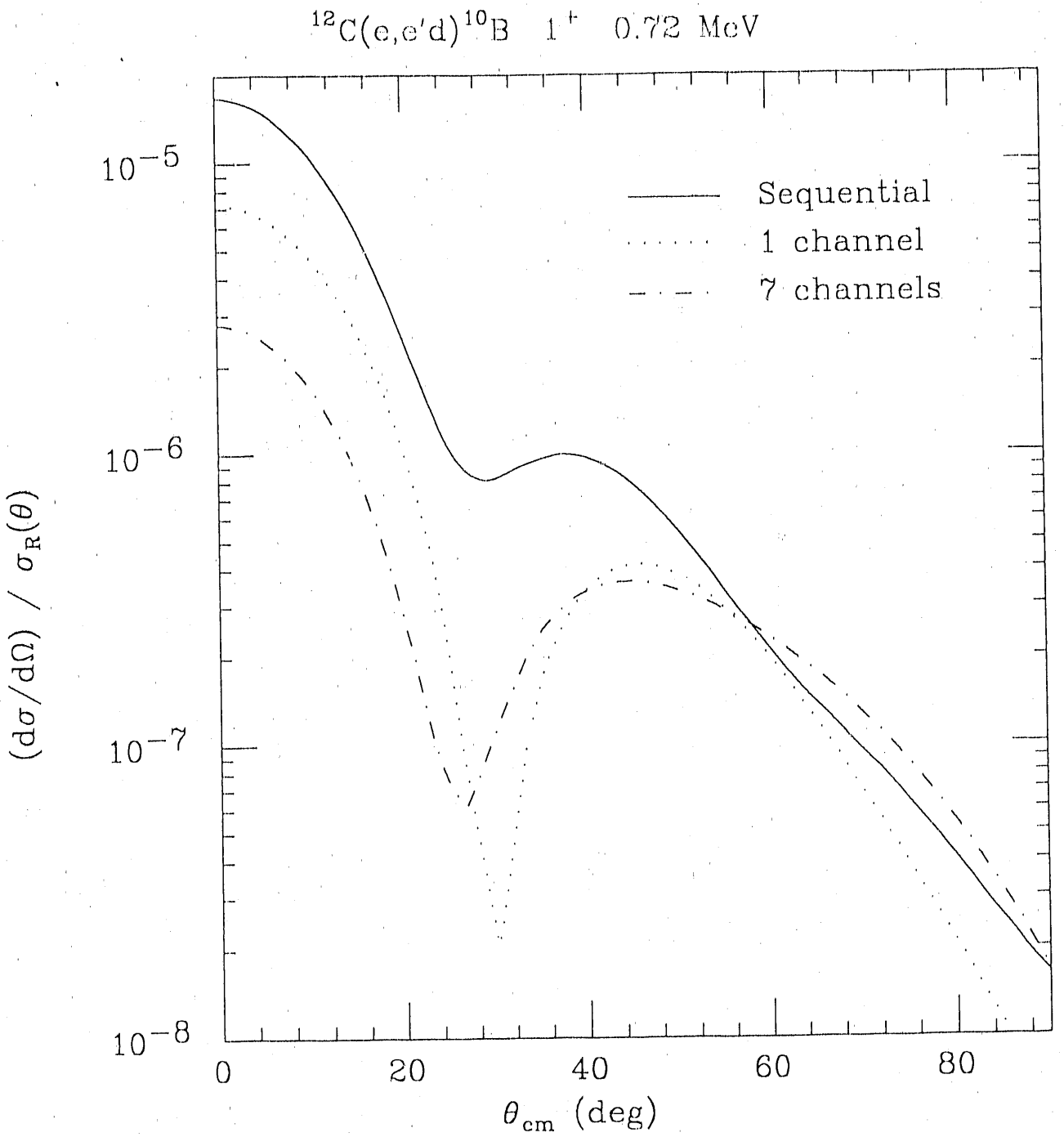

Fig. 2. The sequential knockout model without off-shell corrections compared to the 1 channel and 7 channel cases for the continuum model.

10. Sea Contributions in Dirac RPA for Finite Nuclei J.R. Shepard, C.E. Price, E. Rost and J.A. McNeil

Quantum hadro-dynamics (QHD) is a relativistic quantum field theory of nuclear dynamics[1]. One of the features which distinguishes it from non-relativistic formulations is the presence of a negative energy sea of nucleons which can interact dynamically with positive energy nucleons and thereby affect nuclear properties. The earliest formulations of QHD simply ignored sea effects; these are referred to as mean-field theory (MFT) treatments. Later studies examined sea contributions at the one-loop level for nuclear matter[2] and—utilizing the nuclear matter results in a local-density approximation (LDA)—for finite nuclei.[3] These models constitute the relativistic Hartree approximation or RHA. After independent adjustment of model parameters, both MFT and RHA calculations yield reasonable descriptions of nuclear ground states and are both characterized by the near cancellation of strong attractive scalar (σ) and repulsive vector (ω) fields. RPA descriptions of the nuclear response based on the MFT ground states have been developed by several authors[4] including our group.[5] This MFT-RPA has been shown to possess many appealing features including exactly conserved transition currents and correct treatment of spurious 1^- $T = 0$ excitations arising from violation of translational invariance in the ground state. In addition, it has been shown to provide quantitatively accurate descriptions of low-lying collective excitations in light to medium closed-shell nuclei.

The RPA based on the RHA ground state has been less well studied. However, it has been clear for some time that correlations involving negative energy nucleons—which can be treated in the RHA-RPA—are critical in describing, e.g., the elastic magnetic response of odd-A nuclei at momentum transfers $q \geq 300$ MeV/c. It has also been observed that the longitudinal (e,e') response of nuclear matter is appreciably quenched in the RHA-RPA which in turn affects, e.g., the Coulomb sum rule. Again, the sea contributions tend to improve the correspondance between theory and experiment. More recently, Horowitz and Piekarewicz[6] have employed the LDA to compute the RHA-RPA (e,e') quasielastic response of the finite nuclei ^{12}C and ^{40}Ca. Here again, the sea contributions appeared to have a salutary effect on the calculations, at least for ^{40}Ca. Finally, Piekarewicz[7] has reported RHA-RPA calculations for some of the same low-lying collective states discussed above in connections with the MFT-RPA. Here the results are not encouraging since many of the nice features of the MFT-RPA such as exact current conservation and proper handling of spurious translational modes are lost due to the LDA. Furthermore these levels become much less collective than they are in either the MFT-RPA or in nature.

In order to understand better the role of the negative energy sea in the response of finite nuclei, we have extended our non-spectral Dirac MFT-RPA[5] to include vacuum polarization effects at various levels of approximation beginning with the extreme LDA of Refs. 6 and 7. Our calculational approach is based on the derivative expansion method which has been frequently employed in the RHA description of the ground states of finite nuclei.[8,9] In our version of the RHA-RPA, we emphasize consistancy between the ground state (or, more specifically, the single particle basis) and the RPA. Because the derivative expansion is still an approximation to the exact renormalization of the finite system (see, e.g., Ref. 10), inconsistancies cannot be entirely eliminated as they are in MFT-RPA.

The derivation of the derivative expansion method for the treatment of one-loop vacuum contributions in QHD has been given in many places. We present here the important results required for development of our RHA-RPA following most closely the discussion in Ref. 11. The one-loop effective action is given by

$$\Gamma = \Gamma_{occ} + \Gamma_{vac} + \Gamma_{meson} + \Gamma_{ctc} \tag{1}$$

where Γ_{occ} is the contribution from the positive energy nucleons, Γ_{meson} comes from the free meson part of the Lagrangian and Γ_{ctc} is the contribution from counter-terms. The negative energy sea contribution is

$$\begin{aligned}\Gamma_{vac} &= \int d^4x \Big[-i\mathrm{Tr}\ln\big(i\gamma_m u\partial^\mu - m^* - g_\omega\gamma_m u V^\mu\big)\Big] \\ &\simeq \int d^4x \Big[-U_{eff}(\phi) + \tfrac{1}{2}Z_{1S}(\phi)\partial_\mu\phi\partial^\mu\phi + \tfrac{1}{2}Z_{2S}(\phi)(\Box\phi)^2 \\ &\qquad + \tfrac{1}{4}Z_{1V}(\phi)F_{\mu\nu}F^{\mu\nu} + \tfrac{1}{2}Z_{2V}\big(\partial_\alpha F^{\alpha\mu}\big)\big(\partial^\beta F_{\beta\mu}\big)\Big]\end{aligned} \tag{2}$$

where $m^* = m + S = m - g_\omega\phi$, g_ϕ (g_ω) is the $\sigma NN(\omega NN)$ coupling constant, and ϕ (V^μ) is the scalar (vector) field. As shown in Ref. 10, the coefficients of the derivative terms are proportional to the coefficients of a q^2 expansion of the renormalized vacuum polarization insertions, $\Pi_{V,\sigma}$ and $\Pi_{V,\omega}$. Specifically

$$\begin{aligned} Z_{1S} &= -\Pi^1_{V,\sigma}, \qquad & Z_{2S} &= -\Pi^2_{V,\sigma} \\ Z_{1V} &= +\Pi^1_{V,\omega}, \qquad & Z_{2V} &= +\Pi^2_{V,\omega} \end{aligned} \tag{3}$$

where Π^j is the coefficient of $(q^2)^j$.

The equation of motion for the scalar field is found by requiring that the variation of the total action with respect to ϕ vanish. We express this field as $\phi = \phi_0 + \tilde{\phi}$ where ϕ_0 is the uniform solution for the value of m^* at the point in

r-space about which we make our derivative expansion and $\tilde{\phi}$ is the variation from ϕ_0. Working to second order in $\tilde{\phi}$, the equation of motion for ϕ is,

$$-\Big(1-\Pi^1_{V,\sigma}\Big)\nabla^2\phi+\Big(m_\sigma^2+\frac{\partial^2\mathcal{E}_V}{\partial m^{*2}}\Big)\phi=g_\sigma\Big(\rho_{D,\sigma}+\rho_{V,\sigma}\Big)+\frac{\partial^2\mathcal{E}_V(m^*)}{\partial m^{*2}}\phi$$
$$=g_\sigma\Big[\rho_{D,\sigma}+\rho_{V,\sigma}-(m^*-m)\Pi_{V,\sigma}(m^*0)\Big] \tag{4}$$

where

$$\mathcal{E}_V(m^*,\Lambda)=-\lambda\int\frac{d^3k}{(2\pi)^3}\theta(\Lambda-k)\sqrt{k^2+m^{*2}}$$

is the *unrenormalized cutoff* energy density of the *uniform* sea including all levels with $|\vec{k}|=k\leq\Lambda$. Here λ=4 is the spin-isospin multiplicity of the sea. Note that we have dropped the $Z_{2\sigma}$ and $Z_{2\omega}$ terms. The analogous equation of motion for the (time-like) vector field is

$$-\Big(1-\Pi^1_{V,\omega}\Big)\nabla^2V^0+m_\omega^2V^0=g_\omega\rho_B \tag{5}$$

where ρ_B is the baryon density. The equation of motion for the nucleons is, as usual,

$$\Big[i\vec{\gamma}\cdot\vec{\nabla}-(m+S)-\gamma^0V\Big]\psi=E\psi \tag{6}$$

where $S=-g_\sigma\phi$, $V=g_\omega V^0$ are the scalar and vector potentials, respectively. Solving equations (4) through (6) self-consistently yields the derivative expansion RHA (or RHA/DE[11]) for closed shell nuclei.

We now construct our RHA-RPA based on the RHA/DE. Following Horowitz and Piekarewicz[6,12],we write the full, renormalized RHA-RPA polarizaion insertion as

$$\Pi_{RHA-RPA}=\Pi_0+\Pi_0D_0\Pi_{RHA-RPA}=\alpha\Pi'\alpha+\alpha\Pi_V \tag{7}$$

where $\Pi_0=\Pi_D+\Pi_V$ is the free polarizaion insertion consisting of Π_D due to positive-energy nucleons and Π_V is the renormalized sea contribution. Also, the intermediate polarization Π' is given by

$$\Pi'=\Pi_D+\Pi_DD'\Pi' \tag{8}$$

where the (generalized) vacuum-dressed meson propagator D' is given in terms of

the bare propagator D_0 by

$$D' = D_0 + D_0 \Pi_V D' = D_0 \alpha \tag{9}$$

or

$$D' = \frac{1}{1 - D_0 \Pi_V} D_0. \tag{10}$$

A measure of consistency with our RHA/DE ground state is acheived by making a q^2 expansion of Π_V in the equation for D' and keeping only those terms with counterparts retained in the derivation of the σ and ω equations of motion, Eqs. (4) and (5). We thus go to order q^2 and write, e.g., the vacuum-dressed σ-propagator as

$$\begin{aligned} D'_\sigma(q^2, m^*) &= \frac{1}{q^2 - m_\sigma^2 - \Pi_V(q^2)} \simeq \frac{1}{(1 - \Pi^1_{V,\sigma})q^2 - (m_\sigma^2 + \Pi^0_{V,\sigma})} \\ &= a_\sigma \frac{1}{q^2 - \mu_\sigma^2} \end{aligned} \tag{11}$$

where

$$\begin{aligned} a_\sigma &= a_\sigma(m^*) \equiv \left(1 - \Pi^1_{V,\sigma}\right)^{-1} \\ \mu_\sigma^2 &= \mu_\sigma^2(m^*) \equiv a_\sigma(m^*)\left[m_\sigma^2 + \Pi^0_{V,\sigma}\right] \end{aligned} \tag{12}$$

Similarly, for the vacuum-dressed ω propagator,

$$\begin{aligned} D'_\omega(q^2, m^*) &\simeq a_\omega \frac{1}{q^2 - \mu_\omega^2} \\ a_\omega &= a_\omega(m^*) \equiv \left(1 - \Pi^1_{V,\omega}\right)^{-1} \\ \mu_\omega^2 &= a_\omega(m^*) m_\omega^2 \end{aligned} \tag{13}$$

The expansions of D'_σ and D'_ω through order q^2 are quite accurate for all relevant values of m^* up to at least $q^2 = -(500\ \mathrm{MeV/c})^2$ where the departure from the exact results are still less than $\sim 3\%$. These dressed propagators are now simple Yukawas whose ranges ($\propto \mu^{-1}$) and strengths ($\propto a/\mu^2$) depend on the local value of m^*. This result is numerically convenient since Eq. (8) can now be solved for the intermediate polarization insertion Π' using techniques nearly identical to those employed[5] for the MFT-RPA. The only modifications are, (i) a Slater expansion of the effective Yukawas is required at each grid-point (i.e., for each value of m^*) and, (ii), calculation of the nuclear response contained in $\Pi_{RHA-RPA}$ requires additional foldings of Π' with α.

To make contact with the previous work of Horowitz and Piekarewicz,[6,7,12] we first observe that their RPA calculations are performed in momentum space and, hence, in effect, *all orders* of the q^2 expansion of the vacuum polarization insertions are retained *in the solution of the RPA equation.* Inconsistencies arise because the RHA ground state (or single particle basis) is computed in r-space using the extreme LDA where, e.g., the σ equation of motion comparable to that given in Eq. (4) is reduced to

$$\left(-\nabla^2 + m_\sigma^2\right)\,\phi = g_\sigma\left[\rho_{D,\sigma} + \rho_{V,\sigma}\right]. \tag{14}$$

i.e., not even the leading order contributions to the vacuum polarization insertions enter into the *determination of the basis.* Note that Eq. (14) even differs from the uniform solution in that the "vestigial" $-\nabla^2\phi_0$ term is retained in the former where it contributes due to the non-uniformity of $\rho_{D,\sigma}$ and $\rho_{V,\sigma}$. As shown by Perry[8] and also by Wasson,[9] the additional derivative expansion corrections can be appreciable in finite systems which means that consistency is likely to be more than a formal nicety. Our RHA/DE ground state calculations—which differ in some details from those of Perry and of Wasson—are in progress and will be compared with various other calculations including extreme LDA as employed by Horowitz and Piekarewicz.

1. B.D. Serot and J.D. Walecka, Adv. in Nucl. Phys. **16**, 1 (1986)
2. S.A. Chin Ann. Phys. (NY) **108**, 301 (1977)
3. C.J. Horowitz and B.D. Serot, Phys. Lett. **B140**, 181 (1984)
4. R.J. Furnstahl, Phys. Lett. **152B**, 313 (1985); R.J. Furnstahl, Phys. Rev. **C38**, 370 (1988); P.G. Blunden and P. McCorquodale, Phys. Rev. **C38**, 1861 (1988)
5. J.R. Shepard, E. Rost and J.A. McNeil, Phys. Rev. **C40**, 2320 (1989)
6. C.J. Horowitz and J. Piekarewicz, Nucl. Phys. **A511**, 461 (1990)
7. J. Piekarewicz, Nucl. Phys. **A551**, 507 (1990)
8. R.J. Perry, Phys. Lett. **B182**, 269 (1986)
9. D.A. Wasson, Phys. Lett. **210B**, 41 (1988)
10. P.G. Blunden, Phys. Rev. **C41**, 1851 (1990)
11. R.J. Furnstahl and C.E. Price, Phys. Rev. **C40**, 1398 (1989)
12. C.J. Horowitz and J. Peikarewicz, Phys. Rev. Lett. **62**,391 (1989)

11. Momentum Cutoffs in the Sea J.R. Shepard, C.E. Price, E. Rost and J.A. McNeil

As emphasized in the preceding section, QHD is distinguished from non-relativistic approaches, at least in part, by the fact that the formalism implies the existence of a dynamically interacting negative energy sea of nucleons. The *physical* relevance of this sea is being hotly debated. Most of the controversy has focussed on the fact that, on a small enough length scale, the compositeness of the nucleon must be reckoned with in a way that QHD—which supposes the nucleon to be a fundamental, point-like Dirac field—does not encompass.[1–3] Although such questions are still largely unresolved, there are ample warnings that a "literal" interpretation of the QHD sea is problematic. Perhaps the most striking example is the evidence, based on the huge two-loop corrections to the QHD nucleon self-energy,[4–6] that the loop expansion is badly divergent. Even at the one-loop level of the present work, it has long been known[7–9] that vacuum instabilities arise at space-like momentum transfers of $|\vec{q}| \sim 3$ GeV/c. In the context of the work discussed above, these instabilities are manifested as poles in the vacuum-dressed meson propagators.

With these issues in mind, we have examined at least one alternative to the "literal" treatment of sea contributions discussed so far. This approach employs a momentum cutoff in the sea, retaining contributions only from negative energy states with 3-momentum less than Λ, the cutoff momentum. A "literal" treatment of the vacuum corresponds to taking the limit $\Lambda \to \infty$ i.e., including *all* of the sea. This limit is a questionable one, if for no other reason, because we associate contributions from very high momentum negative energy nucleons with very short distance scales where nucleon compositeness must surely play an essential role. QHD ignores this compositeness and therefore can only be expected to describe the physics down to the scale set by compositeness which must correspond to an inverse length of a few nucleon masses *at most*. Since contributions from this length scale are surely unphysical, QHD *as a nuclear phenomenology*, may make more physical sense with cutoffs, Λ, of the order of a few GeV. Imposing such a cutoff is straightforward calculationally. We simply evaluate $U_{eff}(\phi)$, $\Pi_{V,\sigma}$, $\Pi_{V,\omega}$ or the coefficients of their various expansions with finite Λ, performing the counterterm subtractions numerically.

The cutoff Λ is now an additional parameter in the theory, the variation of which takes us continuously from the MFT ($\Lambda = 0$) to the RHA ($\Lambda = \infty$) limit. For any given cutoff, we must readjust the remaining free parameters of the model—usually g_σ^2, g_ω^2 and m_σ—to reproduce fixed nuclear properties. Table I lists five such parameter sets. The first four were adjusted to yield $BE/N = -15.75$ MeV

at a saturation density corresponding to $k_F = 1.30$ fm^{-1} and to yield 3.48 fm for the RMS charge radius of ^{40}Ca. The fifth set gives $k_F = 1.33$ fm at saturation and reproduces the most recent value[10] of 3.45 fm for the ^{40}Ca charge radius. The differences between the extreme local density[11–14] (RHA/ELDA) and derivative expansion (RHA/DE) parametrization[15] are relevant only in finite systems since the ratios g_σ^2/m_σ^2 and g_ω^2/m_ω^2 are identical for the two parameter sets. As anticipated, these ratios for the last two cutoff (RHA/CO-DE) parameter sets are roughly midway between the MFT and $\Lambda = \infty$ RHA values. The same is true for the nuclear matter m^*/m ratios. The value of the cutoff parameter $\Lambda = 2M_p$ in the RHA/CO-DE is consistent with the general arguments at the beginning of this section and roughly optimizes the description of the spin-orbit splitting of single particle levels which is typically overestimated in the MFT and underestimated in the usual $\Lambda = \infty$ RHA. (Recall that the strength of the spin-orbit interaction roughly scales with the departure of m^*/m from unity.) The exact value of this cutoff is, however, arbitrary and was set to twice the bare nucleon mass for convenience.

Some of the motivation for pursuing the cutoff model presented here emerges from the cutoff dependence of, e.g., U_{eff} and $\rho_{V,\sigma}(m^*,\Lambda) = \frac{\partial \mathcal{E}_V(m^*,\Lambda)}{\partial m^*}$. We find that U_{eff}, $\rho_{V,\sigma}$ and $\Pi^0_{V,\sigma}$ have their largest contributions from sea states with $|\vec{k}| >> 2M_p$ while $\Pi^1_{V,\sigma}$ and $\Pi^1_{V,\omega}$ are augmented by a mere 20% by these same contributions. These dependences are intriguing because, with a cutoff of $\sim 2M_p$, the RHA/CO-DE calculations of ground state properties can be expected to be very similar to MFT results, but the vacuum polarization contributions to the vector polarization insertion will be largely the same as in the $\Lambda \rightarrow \infty$ limit. Thus there is at least the *promise* of a model which possesses the *best* features of both the MFT and the usual $\Lambda \rightarrow \infty$ RHA. The desireable features of the MFT to which we refer are the strong spin-orbit splitting and the high degree of collectivity in the RPA for low-lying collective levels. Those of the $\Lambda \rightarrow \infty$ RHA are the quenching of the transverse (vector) response at moderate momentum transfers; i.e., the quenching of the "front-flow". Cutoff vacuum RPA calculations are in progress; they will show the extent to which this promise is fulfilled.

Table I. Parameters of the Calculations

Calc	$k_F(fm^{-1})$	Λ	m_σ	g_σ^2	g_ω^2	m^*/m
MFT	1.30	0	520	109.7	190.6	0.54
RHA/ELDA	1.30	∞	458	54.3	102.8	0.73
RHA/DE	1.30	∞	550	78.3	102.8	0.73
RHA/CO-DE1	1.30	$2M_p$	635	138.8	154.8	0.62
RHA/CO-DE1	1.33	$2M_p$	610	122.6	147.5	0.62

1. S.L. Brodsky, Comments Nucl. and Part. Phys. **12**, 213 (1984)
2. J.W. Negele, Comments Nucl. and Part. Phys. **14**, 303 (1985)
3. I. Zahed, Phys. Rev. **C37**, 409 (1988)
4. R.J. Perry, in *Proceedings of the Internation Conference on Spin Observables of Nuclear Probes*, C.J. Horowitz, C.D. Goodman and G.E. Walker, eds., Plenum, N.Y., 1989
5. R.J. Perry and D.A. Wasson, in *Nuclear and Particle Physics on the Light Cone*, M.B. Johnson and L.S. Kisslinger, eds., World Scientific, Singapore, 1989
6. R.J. Furnstahl, R.J. Perry and B.D. Serot, Phys. Rev. **C40**, 329 (1989)
7. R.J. Furnstahl and C.J. Horowitz, Nucl. Phys. **A485**, 632 (1988)
8. T.D. Cohen, M.K. Banerjee and C.-Y. Ren, Phys. Rev. **C36**, 1653 (1987)
9. R.J. Perry, Phys. Lett. **B189**, 489 (1987)
10. H. DeVries, C.W. DeJager and C. DeVries, Atomic Data and Nuclear Data Taables **36**, 495 (1987)
11. C.J. Horowitz and B.D. Serot, Phys. Lett. **B140**, 181 (1984)
12. C.J. Horowitz and J. Piekarewicz, Nucl. Phys. **A511**, 461 (1990)
13. J. Piekarewicz, Nucl. Phys. **A511**, 487 (1990)
14. C.J. Horowitz and J. Peikarewicz, Phys. Rev. Lett. **62**,391 (1989)
15. D.A. Wasson, Phys. Lett. **210B**, 41 (1988)

B PUBLICATIONS AND REPORTS – August 1, 1989 to October 1, 1990

1. Published Articles

1. Non-Spectral Dirac RPA for Finite Nuclei, J.R. Shepard, E. Rost and J.A. McNeil, Phys. Rev. **C40**, 2320 (1989).
2. Relativistic Mean Field Theory for Nuclei, A.R. Bodmer and C.E. Price, Nucl. Phys. **A505**, 123 (1989).
3. Correlation Observables in (p,p'γ) Reactions, J. Piekarewicz, E. Rost and J.R. Shepard, Phys. Rev. **C41**, 2277 (1990).
4. Coulomb-Nuclear Interference in Pion Inelastic Scattering, P.D. Kunz, D.S. Oakley and C.L. Morris, Phys. Rev. **C41**, 1081 (1990).
5. $^3P_0$ and $^3S_1$ Contributions to Strange Baryon Interactions, M.A. Alberg, E.M. Henley, L.Wilets and P.D. Kunz, Nucl. Phys. **A508**, 323c (1990).
6. Instability of Infinite Nuclear Matter in the $\sigma - \omega$ Model, C.E. Price, J.R. Shepard and J.A. McNeil, Phys. Rev. **C41**, 1234 (1990).
7. Vacuum Polarization Currents in Finite Nuclei, R.J. Furnstahl and C.E. Price, Phys. Rev. **C41**, 1792 (1990).
8. Instability of Nuclear Matter in the Relativistic Hartree Approximation, C.E. Price, J.R. Shepard and J.A. McNeil, Phys. Rev. **C42**, 247 (1990).
9. Giant Resonance at Complex Excitation Energies, J.R. Shepard, D.S. Oakley and R.J. Peterson, Phys. Rev. **C40**, 2195 (1989).
10. Spin-flip Cross Sections for $^{13}C(\vec{p},\vec{n})^{13}N$(g.s.) at 500 MeV, L.Ray and J.R.Shepard, Phys. Rev. **C40**, 239 (1989).

2. Articles Accepted or Submitted for Publication

1. Dirac RPA Correlations for Ground States of Finite Nuclei, J.A. McNeil, C.E. Price and J.R. Shepard, submitted to Phys. Rev. C.
2. Meson Exchange Current Corrections to Magnetic Moments in Quantum Hadrodynamics, T. Morse, C.E. Price and J.R. Shepard, submitted to Phys. Lett. B.
3. Deformed Chiral Nucleons, C.E. Price and J.R. Shepard, submitted to Phys. Lett. B.

3. Invited and Contributed Papers

1. Second Order Processes in the (e,e'd) Reaction, P.D. Kunz and H.P. Blok, B.A.P.S. **37**, 1812 (1989).

2. Reaction Mechanism and Spectroscopic Results of the (e,e'd) Reactions, R. Ent, H.P. Blok, J.F.J. van den Brand, E. Jans, L. Lapikas, B.L. Berman, W.J. Briscoe, P.D. Kunz and H. Morita, International Conference on Particles and Nuclei, Cambridge Mass., 25-29 June, 1990.

3. $^3P_0$ and $^3S_1$ Contributions to Strange Baryon Interactions, M.A. Alberg, E.M. Henley, L. Wilets and P.D. Kunz, LEAP Stockholm, June, 1990

C. PERSONNEL February 1, 1990 to January 31, 1991

1. Academic and Scientific

P.D. Kunz	Professor
E. Rost	Professor
J.R. Shepard	Associate Professor
C.E. Price	Research Associate
J.A. McNeil	Colo. School of Mines (separate funding)

2. Research Assistants

T. Ferree

END

DATE FILMED

11 / 07 / 90